TECHNICAL UNVIERSITY OF CIVIL ENGINEERING OF BUCHAREST

Faculty of Railways, Roads and Bridges

SCIENTIFIC REPORT NO. 1 "Cable vibration mitigation devices used in cable stayed bridges"

Scientific coordinator: Prof. Univ. Dr. Eng. Nicolae POPA

PhD Student: Eng. Vlad Daniel URDĂREANU

July 2016

TABLE OF CONTENTS

I. INT	TRODUCTION	3
I.1.	International context	3
I.2.	Phenomena that can induce oscillations in cables	4
I.3.	Criteria for determining the vulnerability of cables to vibrations	ç
II. SO 11	LUTIONS AND SYSTEMS USED TO MITIGATE CABLE OSCILLA	ATIONS
II.1.	Tuned masses	11
II.2.	Viscous tuned masses	12
II.3.	Cross ties	13
II.4.	External dampers	13
II.5.	Elastic dampers	14
II.6.	Amortizori vâscoşiViscous shock absorbers	15
II.7.	Magneto-rheological dampers	16
	CASE STUDY: DYNAMIC RESPONSE OF A CABLE WITH EXT AMPING SYSTEMS	TERNAL 21
III.1.	Objectives	21
III.2.	The calculation model	21
III.3.	Validation of the calculation model	22
III.4.	Free cable	25
III.5.	Tuned mass dampers	26
III.6.	Cross ties	28
III.7.	Viscous dampers	29
III.8.	Elastomeric dampers	33
IV. C	CONCLUSIONS	38

I. INTRODUCTION

I.1. International context

The continuous increase in the quality of materials and the development of modern construction technologies in the last century has made it possible for the erection of bridge structures with increasingly larger spans and lower deck heights. This type of structures are generally very flexible and slender, making them sensitive to dynamic actions from the environment, such as earthquakes, wind or even live actions from traffic.

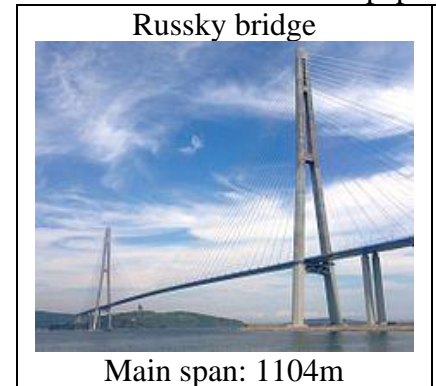
In this context, cables have begun to be used more and more often as structural elements, with multiple applications in the field of civil engineering, such as suspension bridges, cable-stayed bridges, antenna towers, etc.

Cable stayed bridges began to be adopted more and more often after the 1950's, due to easier construction, aesthetics, but also on economic criteria. The principle of this type of structures is to cross large spans with very slender decks by transferring the efforts locally, at multiple points, using cables, and transmitting them to the piers. The tension in the cables can be controlled relatively easily, thus being able to induce an optimal state of stress in the superstructures.

Modern international design practice favors the use of multiple cables with smaller cross-sections and denser anchor points in the deck, which allow easier inspection, maintenance and even replacement under traffic.

Usually, this type of solution includes three spans and two pylons, but there are many examples of single pylon cable-stayed bridges (especially at pedestrian walkways – ex. Bridge over Lake Moghioros) or with multiple pylons (ex. Millau viaduct).

At the time of this paper, the largest spans crossed by cable-stayed bridges are as follows:



Total length: 1885.53m
Total width: 29.50m
Year of completion: 2012



Total length: 1690.00m Total width: 41.00m Year of completion: 2008



Main span: 1018m
Total length: 1596.00m
Total width: 51.00m
Year of completion: 2009

Figure 1 –The largest cable stayed bridges at international level

These solutions could be adopted by ensuring a very efficient use of various stays systems, which are structural elements of high resistance. They are also useful for maintaining a pleasant aesthetic appearance. However, it must be taken into account that these cables are very flexible and have an extremely low internal damping (between 0.25% - 1%) and thus, they are susceptible to dynamic excitation from the outside and can frequently develop vibrations with large amplitudes. This phenomenon is more pronounced in the case of longer cables or with lower tension levels.

At the international level, requirements in recent years have opened the way for increasingly larger spans. This led to more frequent cases of excessive vibration phenomena in cables, which often led to degradation or even collapse of some structural elements. The most

sensitive to these phenomena are not the strands themselves, but their anchorages or protection systems.

In addition to traffic actions, there are a multitude of natural phenomena that can induce oscillations in cables, among which are mentioned: the combination of wind and rain, the shedding of Von-Karman vortices, galloping, wake galloping, ice deposits, etc.

Regarding the deduction of the cause of cable oscillations that led to structural degradations, it was not always possible to identify the disturbing factors of the observed instabilities, as the causes can manifest by themselves or together in multiple combinations. However, the following can be noted:

- At the Ben-Ahin and Wandre bridges in Belgium, oscillation amplitudes of approximately 0.50m respectively of 0.30m were recorded, accompanied by light vibrations of the deck. Although they were initially attributed to the excitation phenomenon due to the combination of wind and rain, it was also found that the oscillations of the superstructure in turn increased the vibrations in the cables. Similar examples of deck-cable interaction leading to larger amplitudes of vibration displacements have also been recorded for the following: Annacis Bridge in Canada, Faro Bridge in Denmark, Helgeland Bridge in Norway, Burlington Bridge in the United States, Second Severn Bridge in Great Britain, etc.
- At the Maracaibo Bridge in Venezuela, more than 500 cables were found to be damaged and required replacement less than 2 years after completion, and another 3 cables were replaced a year later; the cause was underestimating the dynamic phenomena which caused fatigue degradation
- At the Guazu Bridge in Argentina, a cable broke due to corrosion and fatigue; the technical report at the time concluded that part of the fault was due to its large vibration amplitudes at certain wind speeds and directions.
- At the Jinan bridge over the Yellow River in China, all stays were replaced only 13 years after completion; the reason for this is yet to be uncovered
- The Guadiana Bridge in Portugal is a more recent example of a bridge with problems due to cable vibrations; strong vibrations of the cables in interaction with oscillations of the deck were found to be the main reason for the degradations;



Figure 2 – Cable stays degradations

I.2. Phenomena that can induce oscillations in cables

Apart from the base wind speed and aerodynamic instability, there are multiple mechanisms that, depending on various wind speeds, can induce dynamic behavior of cable stayed bridges. In this chapter, four phenomena that introduce problems and should be taken into account in the design of such structures will be presented:

- ➤ Vortex shedding
- ➤ Wake galloping
- Aerodynamic instability due to snow or ice deposits on cables
- > The combination of wind-rain

Reynolds number and vortex shedding

Vortex shedding is an aeroelastic phenomenon found in fluid dynamics. This is an oscillating flow regime that occurs when a fluid (such as air) moves past cylindrical bodies at certain speeds. Vortices are formed behind the object, which are periodically detached on one side and the other of it.

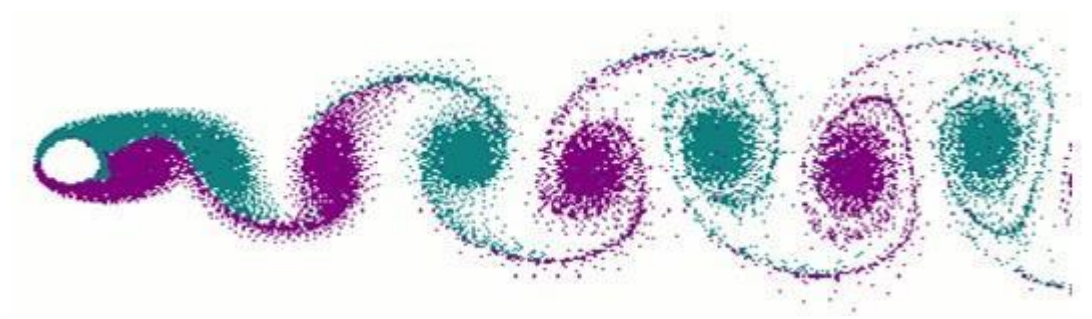


Figure 3 – The path of fluid particles at vortec shedding

As the fluid approaches the surface of the cylinder, the pressure level rises from the value corresponding to free flow, to the stagnation point at its top, corresponding to the highest pressures. Pressure forces tend to push the fluid particles to one side or the other of the cylinder, forming boundary layers. The forces generated at the surface of the body are countered by the forces in the viscosity of the fluid, which cannot flow all the way to the back. The boundary layers detach on both sides, forming 2 shear layers. Particles from the rigid surface move more slowly than those from the outside, resulting in relative rotations between them, which can lead to the appearance of vortices.

Along with vortices, alternating areas of low pressure appear downstream of the body, which tend to move towards points of lower pressure.

If the cylinder is flexible, or not well fixed, and if the vortex shedding frequency corresponds to the resonance of the structure, it can oscillate harmonically with ever-increasing amplitudes, as energy is introduced into the system. Due to their long lengths and their insignificant bending stiffness, the cables are very sensitive elements to such phenomena that induce excitations in their transverse direction.

Wake galloping

Wake galloping is the phenomenon by which the oscillations of a downstream cylinder are induced by the turbulent flow in the wake of another one located upstream. Considering 2 cylinders located a few diameters apart in the flow direction as in Figure 4, the circulation flow in of the first one is rotationally clockwise at the top and counter-clockwise at the bottom. For this reason, the downstream cylinder, if left free, will describe an elliptical trajectory as shown in the figure.

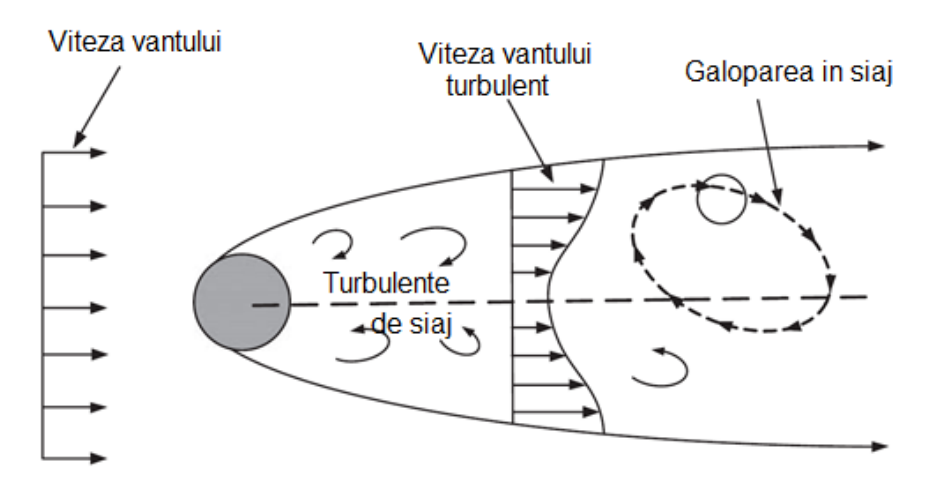


Figure 4 – Wake galloping

Wake galloping can occur at the cables of stayed bridges or at the hangers of suspended ones. It happens at high wind speeds and usually leads to large amplitude oscillations.

However, the phenomenon occurs provided that the natural period of vibration of the downstream cable is large compared to the vortex shedding periods of both the front and rear cylinders. In such conditions, when the distance between the 2 cylinders is in the limit of several diameters, the downstream one enters a zone of instability when galloping. Research shows that this region of instability is approximately 8 to 20 cable diameters.

Galloping induced by the wind-rain combination

The wind-rain combination vibration inducing phenomenon is the most common dynamic excitation phenomenon in cables of cable-stayed bridges. It was first reported by engineer Hikami when the pylons of the Meiko-Nishi Bridge in Japan showed vibrations of unacceptable amplitudes. At the time, the most curious thing was that they were observed only in certain windy conditions, but always when it was raining. The recorded oscillations increased up to a level of approximately 2 times the outer diameter of the stay, i.e. approximately 28cm and at wind speeds between 8-14 m/s. The frequency of motion was about 1-3 Hz, well below the Strouhal frequency for excitations under vortex shedding, and the cables were too far apart to have aerodynamic interference. In this context, it was concluded that it was a completely new phenomenon compared to those known at that time.

After reporting this phenomenon of dynamic excitation, it became clear that vibrations had been observed in other structures as well in the past, occurrences that could be classified under the same category. Some of these are as follows:

- Kohlbrand bridge, Germany, 1974
- Brottonne bridge, France, 1977
- Meiko Nishi bridge, Japan, 1984
- Faro bridge, Denmark, 1985
- Tempozan bridge, Japan 1986
- Aratsu bridge, Japan 1988
- Ben Ahin bridge, Belgium, 1988
- Burlington bridge, Vermont-USA, 1990
- Glebe Island bridge, Australia, 1990
- Nampu bridge, China, 1992
- Yangpu bridge, China, 1995
- Erasmus bridge, Holland, 1996
- Orsund bridge, Denmark-Sweden, 2001
- Cochrane bridge, Alabama-USA, 2002

The combination of rain and moderate speed wind can cause oscillations in cables with large vibration amplitudes and periods. This phenomenon has been observed in many cable-stayed bridges and has been vastly studied.

Over time, a lot of research has been carried out on this phenomenon, including field measurements, wind tunnel tests or analytical models. It was found that these oscillations occurred especially when there was rain and moderate wind speed between 8-15 m/s, in a direction of 20°-60° to the plane of the cable, with the stay inclined to the direction of the wind. The recorded periods were greater than 0.33s, and the maximum amplitudes between 0.25m-1.00m, resulting in violent movements that even led to adjacent cables hitting each other.

Wind tunnel tests have shown the main component of this aeroelastic instability phenomenon to be the formation of rivulets along the upper and lower surface of the cables. These change the outer aerodynamic shape of the cable's sheath and move as the cable oscillates, resulting in the induction of additional vibrations from the wind. The range of velocities that proved most favorable for this phenomenon was found to be in a range that kept the stream in the upper part of the stay within a certain critical zone on the upper surface. It was also observed that the level of these oscillations is reduced to an insignificant level when the corresponding Scruton number is greater than 10.

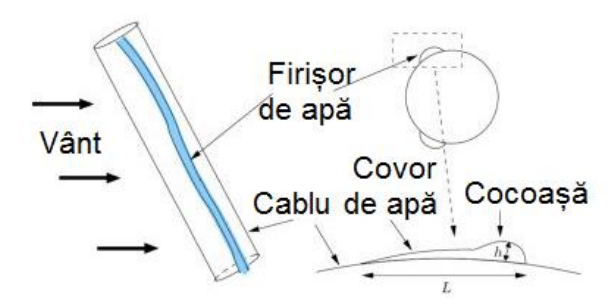


Figure 5 –Water rivulets forming on cables

Wind-rain induced oscillations, are an important phenomenon to be considered in the design of cable-stayed bridges and vibration damping systems due to their large amplitudes and frequent recurrences.

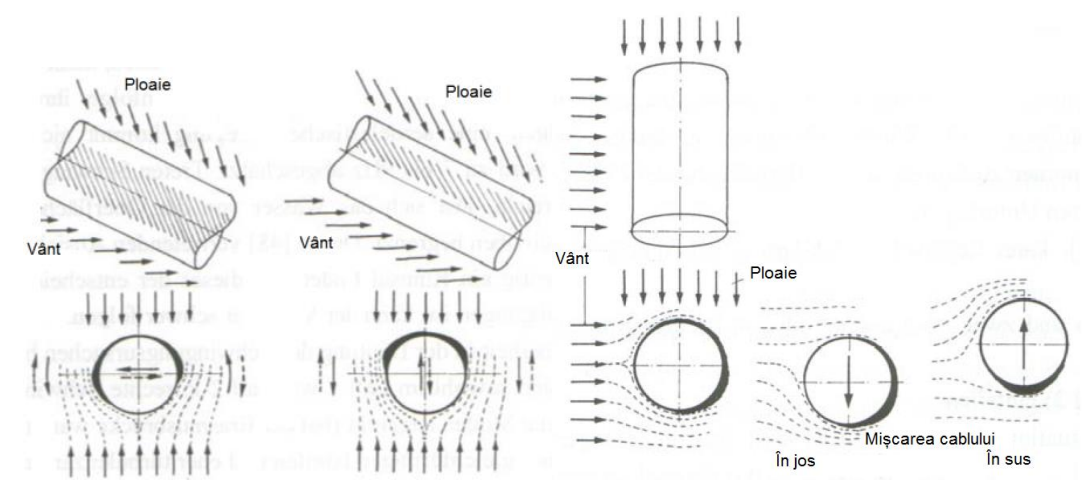


Figure 6 –Oscillations in cables from wind-rain combination

In order diminish the effect of this phenomenon, in addition to internal or external damping systems, a helical-shaped wire mounted on the outer surface of the sheath can be used. This has the role of modifying the course of the streams and reducing their effect to a large extent.

Deposits of ice or snow on cables manifest similarly to the phenomenon of induction of oscillations from the combination of wind and rain, but at much lower temperatures. Due to wind, precipitation and low temperature, deposits (snow or ice) begin to accumulate on the outer surface of the cable.

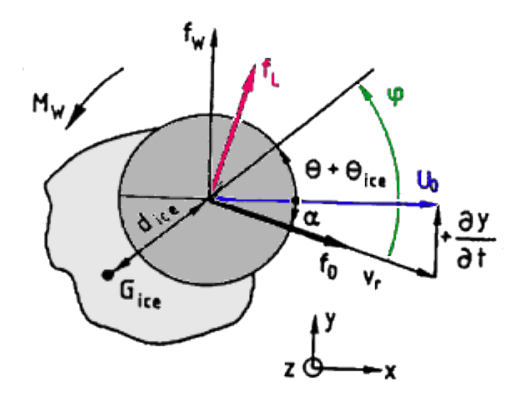


Figure 7 – Schiță cu depunerea gheții

Unlike the wind-rain combination where the accumulated water runs down the cable, in this case the material deposited on the surface is static. This means that the volume accumulated on the side surface is much larger and the galloping effect manifests in a more turbulent manner.

An important aspect to be aware of is that deposits introduce an eccentric weight on the stays, which at some point can increase so much as to cause it to twist. Thus, the shape of the object placed in the flow stream is constantly changing, and the effect on the induced oscillations can vary in a more favorable or even unfavorable way.

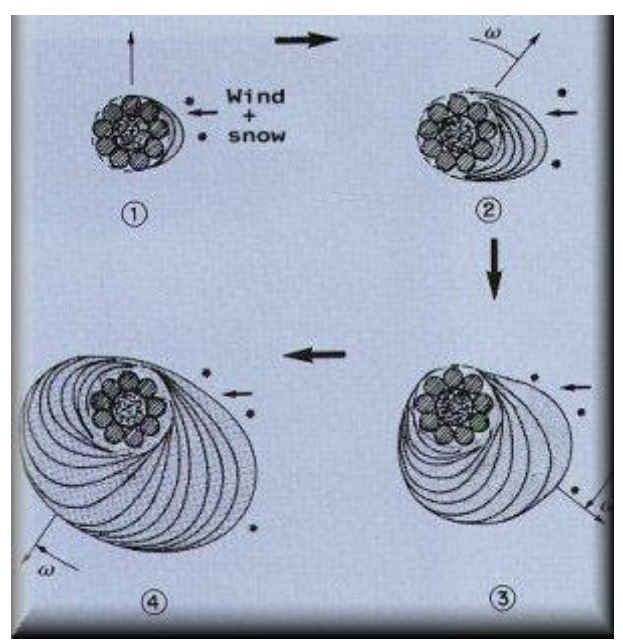


Figure 8 – Snow/ice build-up on cables over time

Unlike the phenomenon of wind-rain combination, for which there are other methods of prevention besides dampers, the buildup of precipitation on cables cannot be reduced by methods other than energy dissipative ones.

The recurrence of the phenomenon of oscillations due to the deposition of snow or ice is encountered much more rarely than that in the case of the combination of wind and rain, but its effects are much more dangerous. In addition to the vibrations induced in the cable, there is the possibility of sudden detachment of the deposits from the outer surface of the cable, which would lead to the induction of a strong impulse on it. As a rule, the detachment occurs at moments of

minimum oscillation and therefore a positive impulse would lead to a sudden but temporary increase in the maximum amplitude.

I.3. Criteria for determining the vulnerability of cables to vibrations

Reynolds number

The flow regime around long circular cylinders perpendicular to the flow direction is highly dependent on the Reynolds number, which enables the forecasting of the following types of flow:

- R_e <5 for small Reynolds numbers the flow regime is stable, laminar, and the currents do not separate
- \gt 5 \le R_e <40 the flow regime is still stable and laminar, and 2 symmetric vortices are formed behind the cylinder, but they do not shed
- > 40≤ R_e <150 as the Reynolds number increases, the wake becomes unstable and vortex shedding begins; initially, one of the vortices described in the previous point detaches, followed by the second and, due to the pressure differences, the process becomes repetitive, with a periodic but laminar current; this phenomenon is called "Karman Vortex Alley"

$$\frac{h}{l} = \frac{1}{\pi} \cdot \sinh \sinh - 1\{1\} = 0.281 \tag{I.1}$$

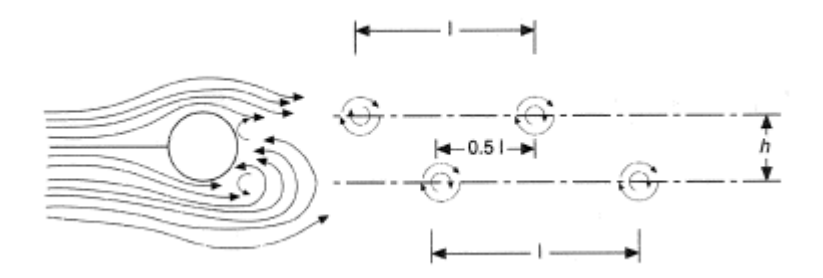


Figure 9 – Vortex shedding

- ➤ $150 \le R_e < 300$ also called the transition zone, this segment is characterized by the appearance of periodic irregular disturbances; the flow regime gradually changes from laminar to turbulent
- $> 300 \le R_e < 3 \cdot 10^5$ zone called critical, characterized by its turbulent, but periodic character, with the formation of strong eddies in its wake; as a side effect, the drag coefficient gradually decreases
- $> 3 \cdot 10^5 \le R_e < 3.5 \cdot 10^6$ supercritical flow segment, where three-dimensional disturbances disturb the periodic formation of vortices; also the wake narrows and becomes disorganized
- > 3,5 · $10^6 \le R_e$ value after which the flow returns to the turbulent regime but with periodic formation of vortices

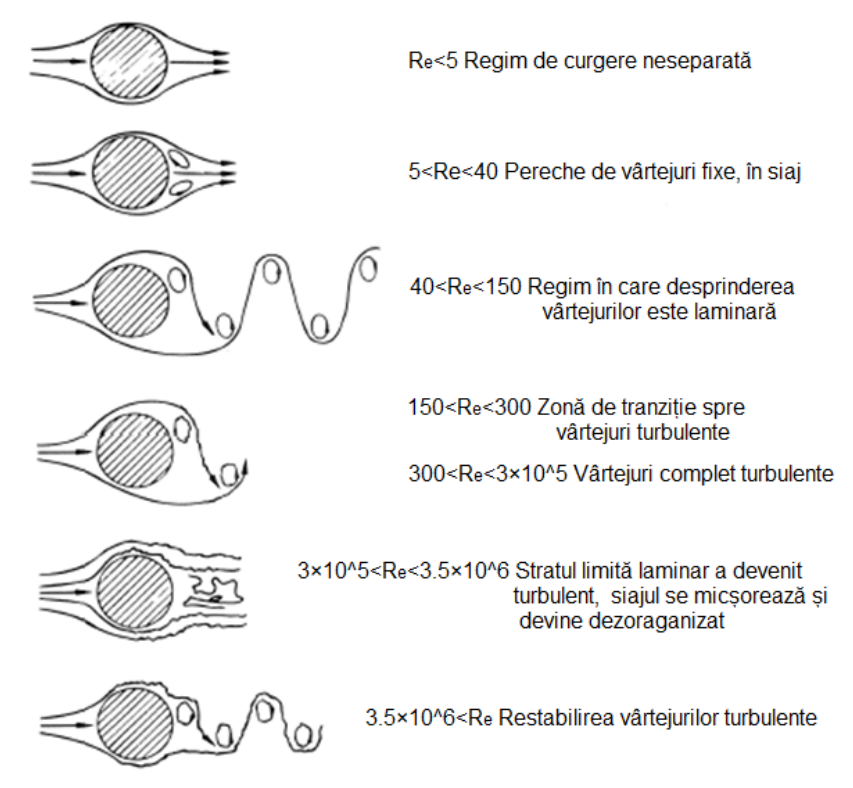


Figure 10 -Influence of the Reynolds number on vortex shedding and flow regime

In addition to these, the Reynolds number can also provide information on vortex shedding frequency as follows:

- For $30 \le R_e < 2 \cdot 10^5$ subcritical regime the vortex shedding period is constant
- For $2 \cdot 10^5 \le R_e < 4 \cdot 10^6$ supercritical regime the vortex shedding period is variable (random)
- ightharpoonup For $4 \cdot 10^6 \le R_e$ hypercritical regime the vortex shedding period is again constant

The Strouhal Number and the "Fixing" phenomenon

In the case of cylinders, the Strouhal number can be taken as 0.2 for a wide range of flow velocities. In this situation, the increase in speed leads to a decrease in the detachment period of the vortices. Thus, the alternation of the vortices induces an almost harmonic transverse force and therefore, the phenomenon of resonance can appear once the structure's first period of vibrations corresponding to the movement in the respective direction is reached. Further increasing the speed will lead to resonance once the next natural period of vibration is reached and so on.

From a theoretical point of view, resonance can occur at any natural period of vibration of the structure. In sufficiently flexible structures, it is possible that the displacement amplitude of the oscillations is large enough to control the vortex shedding phenomenon. This phenomenon is also known as "Fixing". This means that resonance can be maintained over a wider range of speeds. If the wind speed changes enough to leave this zone, the vortices shedding will again be characterized by wind alone.

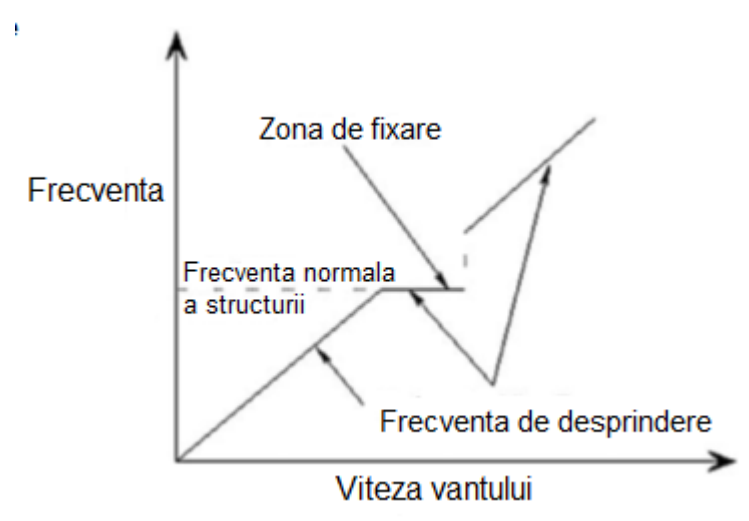


Figure 11 – Graph of velocity over detachment frequency showing the fixing phenomenon

Scruton Number

It is a dimensionless parameter very often used in fluid mechanics to determine the damping of the wind-induced structural response. In general, the damping of wind-induced instability phenomena is achieved by increasing this number.

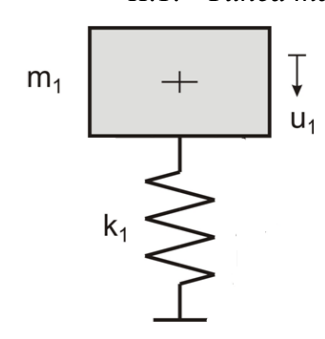
As mentioned in the previous chapter, 95% of cable vibrations are due to the combination of wind and rain. To avoid this phenomenon, it is recommended that the value of the Scruton number for the cable be greater than 10. For the outer surfaces of the cable sheaths with aerodynamic profile, it can be lowered to the value of 5. The Scruton number for a cable is determined by the formula:

$$S_C = \frac{m \cdot \xi}{\rho \cdot D} > 10$$
, where: (I.1)

- m -mass per unit length of the entire cable (including the sheath)
- ξ -damping expressed as a percentage of the critical damping
- ρ air density
- D outer diameter of the cable

II. SOLUTIONS AND SYSTEMS USED TO MITIGATE CABLE OSCILLATIONS

II.1. Tuned masses



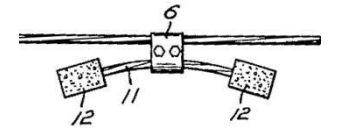
The vibration mitigation system based on tuned mass dampers involves fixing some springs with weights at certain points of the cables. The idea is to modify the dynamic characteristics of the cable (modes of vibrations, periods and natural frequencies of vibration) in order to reduce the effects of the resonance phenomenon.

The main advantages are:

- great endurance in time, because all the components are mechanical and robust
- not influenced by strong temperature variations
- relatively low costs both for the device itself and for its maintenance

Main drawbacks:

- they are effective only for certain ranges of amplitudes and periods of the oscillations, for which they were calculated



- difficult to handle on site, because they are relatively heavy and must be positioned in hard-to-reach places (generally towards the middle of the cables)

Initially, the first models of such devices consisted of 2 concrete blocks linked together by a rod, which in turn was fixed to the cable at a distance that allowed relative movement between it and the weights.



Nowadays, steel masses are used instead of concrete blocks. They are hollow inside and can have different geometric shapes such as: sphere, cylinder, cone, bell. Newer models have unequal weights, which allows them to operate efficiently over a wider range of frequencies.

Their positioning along the cable also depends on the targeted mode of vibration. Areas of maximum amplitude or inflection points should be avoided. The arrangement should theoretically increase the number of half-waves that form in that mode and thus lead to a decrease in peak displacements.

When calculated accurately, built and installed correctly, the masses are very efficient at absorbing unwanted energy from the structure and even dissipate it internally, thus drastically reducing unwanted deformations in the structure and thus, reduces damage taken by the stays.

II.2. Viscous tuned masses

Relatively new technology that involves the introduction of a viscous energy dissipation mechanism inside the given mass.

Currently it has not been implemented in any work, but there is a lot of promising research in the field.

Although the dissipation mechanism cannot be as efficient as that of a classic viscous damper, the position much closer to the center of the cable gives increased efficiency to the device, but for the moment this type of solution is still in the concept stage.

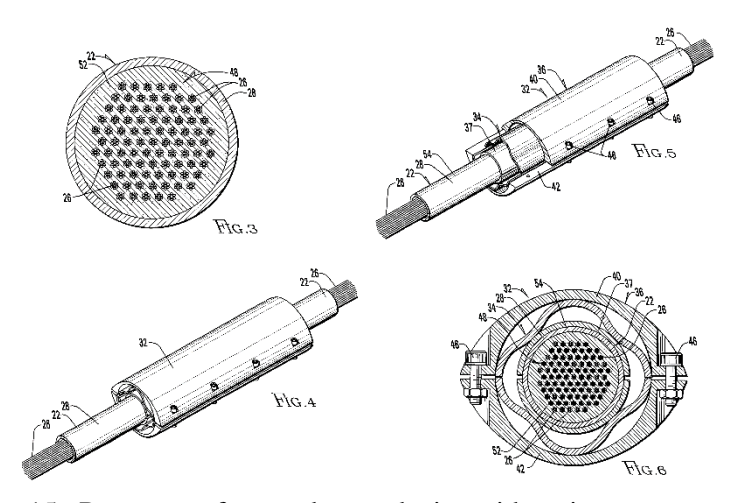


Figure 15 - Prototype of a tuned mass device with a viscous component

II.3. Cross ties

They are transverse braces that connect the main cables to each other at key points or even to the superstructure. The main purpose is to change the deformed shape of the cable to reduce the vibrations by a certain mode of vibration. As a favorable side effect, the fact that the anchor points are on adjacent stays that each have different dynamic characteristics causes them to interact with each other and drive each other out of resonance.

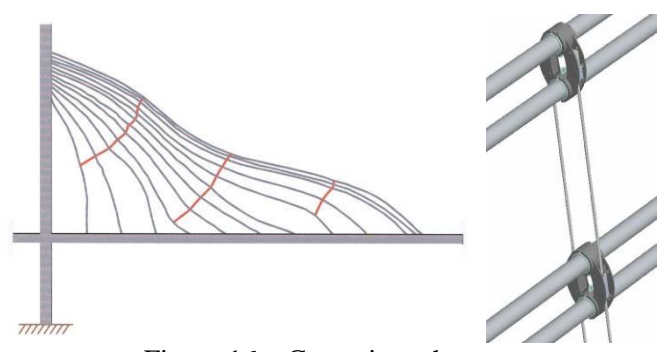


Figure 16 – Cross ties scheme

The first and most famous example of a cable-stayed bridge to adopt this system is the Normandy Bridge over the River Seine in France. It has a main span of 856m, a total length of 2143m and a width of 23.60m. From each pylon towards the spans, there are three sets of cross ties, arranged at equal distances. Their purpose is to guide the oscillations of the stays towards the 4th mode of vibration.



Figure 17 - Cross ties on the Normandy Bridge

When applying these solutions, it must be taken into account that too many cross ties can become unsightly.

Examples of cable-stayed bridges with cross ties:

- Normandy bridge France 1995
- The second bridge over Severn Great Britain 1996
- Oresund bridge Sweden 2000
- Bridge over Charles River USA 2002
- Rion-Antirion bridge Greece 2004
- The new bridge over Cooper USA 2005

II.4. External dampers

The most frequently used method for ensuring a sufficient level of damping in the stays, that avoids degradation of the structural elements, is the attachment of external transverse dampers. They have the role of dissipating the energy in the cables and reducing the vibration amplitudes to an acceptable level. Ideally, they should be attached as close to the center of the cables as possible, but they are usually attached at deck level, about 1%-3% along the length of the cable.

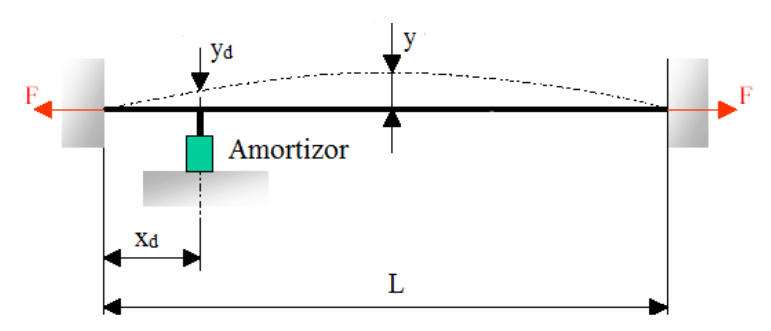


Figure 18-Sketch of cable oscillation with damper attached

Vibration mitigation systems include the attachment of a special device, close to the end of the stays, at deck level, which will reduce the amplitudes to an acceptable level. These devices are also called energy dissipators, a process that involves the generation of a response force in the dampers, which deforms due to the movements in the cable. The product of these two creates mechanical work, which is equivalent to dissipated energy. The energy dissipation capacity per cycle is expressed in the hysteresis of the damper. The larger the area bounded by it, the better the energy dissipation capacity.

Depending on the type of method used, they can be divided into 3 large categories, in order of their efficiency, as follows:

- elastomeric dampers —based on the ability of the special rubbers in their composition to behave under a bilinear law, one elastic and one plastic,
- viscous dampers based on the force generated when a special liquid passes through a piston with special holes at the end
- friction-based dampers based on the force generated on a friction surface when it moves

II.5. Elastic dampers



Elastic dampers reduce cable oscillations by storing and dissipating energy internally in the component materials. This is done by the mechanical work given by internal elastic but especially plastic forces.

Elastic dampers are of two types, namely based on elastomers or based on friction. The first type works by a shear force inside a special elastomer, and the second generates frictional force due to the displacement corresponding to the deformation of the cable.

Their main advantage over other dampers is their smaller size and ease of installation. Their disadvantage lies in the fact that they can only accept small deformations, which greatly reduces their ability to dissipate energy.



The fact that all their damping characteristics are dependent on the properties of the component materials makes these dampers very dependent on the outside temperature. The elastomer becomes very flexible at high temperatures and very rigid at low temperatures. A sudden decrease can even lead to its premature rupture. Also, in the case of those based on friction, the coefficient of friction between the 2 materials is also strongly influenced by the external temperature and the humidity of the environment.

In the following there is a force-deformation graph that shows the behavior of such a device in different stages:

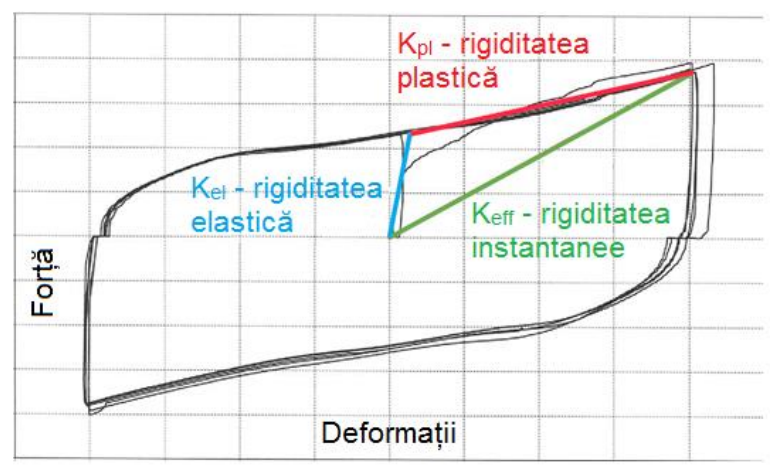


Figure 21 –General force – deformation graph of an elastic damper

As can be seen in the graph, their behavior includes an elastic, shorter sequence, and a longer, plastic one. As the deformations increase, the force also increases suddenly in the first sequence, and much more slowly in the second. It is important to mention that the efficient energy dissipation begins once the formation has entered the plastic stage. Thus, for optimal damping, the elastic resistance must be small enough to allow a quicker entry into the plastic stage, but high enough to achieve sufficient manual work until the maximum deformation is reached. This also shows the fact that these dampers only behave effectively on certain ranges of deformations, being either too flexible or too rigid outside of them.

Calculation formula for the force given by an elastic shock absorber:

$$F = y_d \cdot K_{eff} = y_d \cdot K_{el} + (y_d - y_{el}) \cdot K_{pl}$$
 (IV.1)

II.6. Amortizori vâscosiViscous shock absorbers



Viscous dampers are cylinders with pistons that have holes in the head through which a special fluid is allowed to pass, in order to dissipate energy.

It consists of 2 chambers, separated by the piston head, in which there is a compressible liquid based on silicone. The holes allow the liquid to circulate from one chamber to another

as the piston moves. The force is generated as a result of the pressure difference between the piston head and the compression in the liquid.

Thus, the force given by the damper is dependent on the speed of the piston rather than its deformation. To highlight this, graphs of force over deformation, respectively speed are presented below:

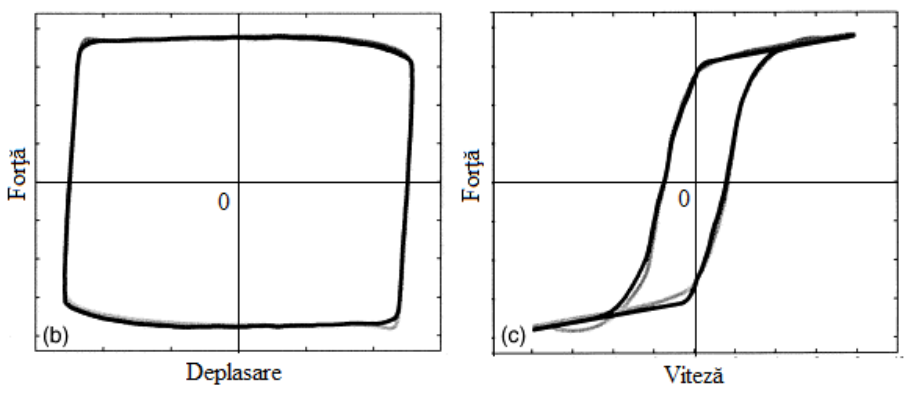
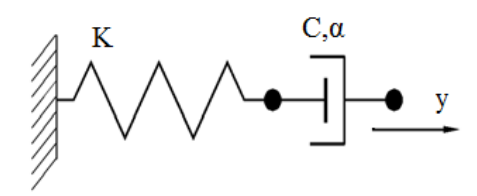


Figure 24 - General force – deformation, respectively force- - speed graphs for viscous dampers

The mathematical model that is the basis of the calculation relationships consists of a spring of stiffness K, connected to a piston of viscosity C.



In addition to these, there is another important factor, which determines the influence of the speed on the freedom of circulation of the liquid from one chamber to another, which is further denoted by α . Depending on this coefficient, the curvature in the force-displacement diagram will be smaller or larger.

According to actual laboratory records, the extreme values for it are 0.15 and 2.

The formula for calculating the force generated by the damper is:

$$F = K \cdot y_d + C \cdot v_d^{\alpha}, \tag{IV.1}$$

Where K is the linear stiffness of the damper, C the viscous coefficient of the liquid, v_d the speed of the piston head and α the speed exponent, characteristic of the liquid.

The optimal viscous coefficient can be determined for each cable and individual vibration mode according to the formula:

$$c_i^{opt} = \frac{1}{i \cdot \pi \cdot \frac{x_d}{L}} \cdot \sqrt{T \cdot m},\tag{IV.2}$$

Where T is the tension in the cable, and m is its mass per linear meter.

Since the external excitation can have different frequencies, the optimal viscosity coefficient does not always correspond to a single mode, but is generally found by interpolating between the first 4-5 modes. This makes determining it a bit more difficult than it might seem at first glance.

Viscous dampers are less affected than elastic ones in terms of weather phenomena. The high pressure inside the liquid causes it to heat up well above the maximum temperatures that can be recorded. However, frost may occur on the outside, which could prevent the movement of the piston.

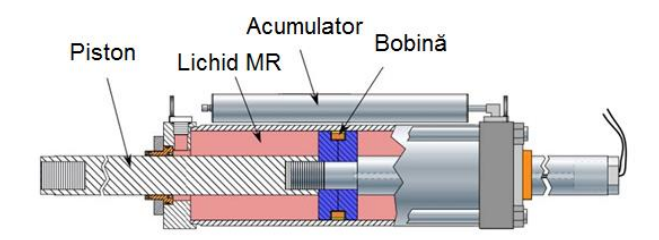
II.7. Magneto-rheological dampers

As shown in the previous chapter, viscous dampers are efficient vibration damping devices, provided that their working parameters are very well predetermined. Tuning these can be done so as to lead to optimal damping, but only for a few modes of vibration of the stays. On site

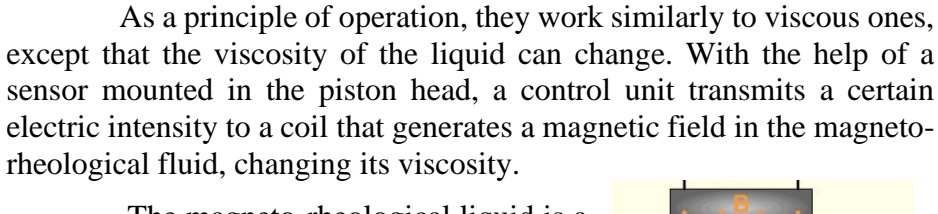
measurements have shown that the vibrations of the first mode are predominant, but also the following 4-5 modes have an important influence on the dynamic response of the cables.

In addition to this, another disadvantage of these devices is the influence of the bending/torsional stiffness of the deck, which is often very small and affects the devices, or the bending stiffness of the anchorage, which can sometimes be large enough to influence the oscillations and should be taken into account. These are reasons why sometimes viscous dampers are not the most efficient damping devices that ensure dynamic stability.

These limitations led to the development of semi-active vibration control systems, namely magneto-rheological dampers, which are similar in operation to viscous dampers, but have the advantage that the internal force given by the device can be adjusted in real time. This allows the devices to function optimally at any level of oscillation amplitudes.



Magneto-rheological dampers are semiactive dissipators that can change their properties using magneto-rheological fluids. They have the ability to change its state from liquid to semisolid in a continuous and fully reversible manner by means of a magnetic field.



The magneto-rheological liquid is a special oil, which, when introduced into a magnetic field, changes its apparent viscosity until it reaches a given visco-elastic stage. More importantly, its resistance can be controlled with great precision by varying the

strength of the magnetic field. Fluid particles are on the order of micrometers and too heavy to undergo Brownian motion. As with viscous dampers, the high temperatures inside it make it very little dependent on outside temperatures

Magneto-rheological dampers can work in passive mode, at a constant current intensity, in which they do not change their properties, or in semi-active mode, in which they constantly change their intensity depending on necessity, the response time being in the order of tens of milliseconds. To better explain this process, the steps taken are presented in the following logical diagram:

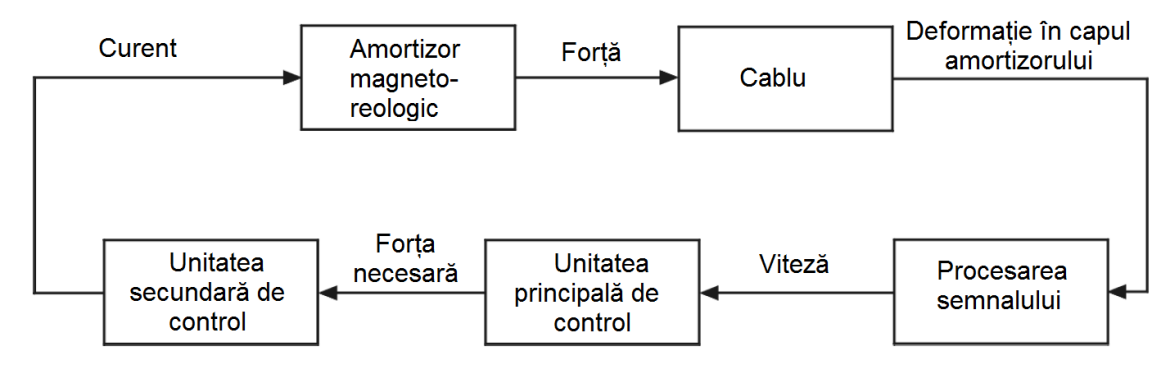
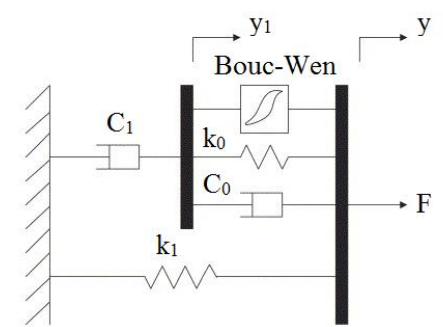


Figure 29 - Logic diagram of the magneto-rheological damper

The mathematical model underlying the calculation of the force in the damper is a little more complex than the rest of the studied devices. It should be remembered that all the constants from the other models are in this case, variables that depend on the intensity of the electric current.



There are several mathematical models that can be used, but the best ones have been obtained using the one shown in the figure. The main dissipative element is the Bouc-Wen component of the assembly, connected in parallel with an elastic spring k_0 and a viscous damper C_0 , all 3 being serial connected with a viscous damper C_1 , this whole assembly being in turn connected in parallel with an elastic spring k_1 .

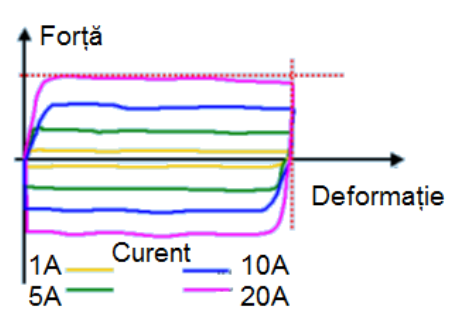
In order to determine the force generated by the shock absorber, the characteristics of the shock absorber depending on the current are considered known and the formulas are used:

$$F = c_1 \cdot \dot{y}_1 + k_1 \cdot (y - y_0) \tag{IV.3}$$

$$\dot{y}_1 = \frac{1}{c_0 + c_1} \cdot (c_0 \cdot \dot{y} + k_0 \cdot (y - y_1) + k \cdot z$$
 (IV.4)

$$z = -d \cdot |\dot{y} - y_1| \cdot z \cdot |z|^{n-1} - g \cdot (\dot{y} - \dot{y_1}) \cdot |z|^n + \alpha \cdot (\dot{y} - \dot{y_1})$$
 (IV.5)

Where y is the total displacement in the piston head, y_1 is the relative displacement in the secondary damper C_1 , and z a variable that helps solve the resulting system of equations.



To better exemplify the mode of operation, the hysteresis curve for different current intensities is presented. This is an ideal representation, but one can see how the most energy is dissipated at the highest intensity. In reality, however, a decrease in intensity is needed along with the amplitudes, in order to maintain an optimal level of cable damping.

The first full-scale prototype magneto-rheological damper was used at the Eiland Bridge near Kampen in the Netherlands. This was done to test their effectiveness or behavior over time and has remained in use to this day.

The cable to which the damper was attached has a length of 163.70m, with a tension of 5082kN and a mass per linear meter of 66.55 kg/m. There is also an elastomeric damper attached

at 2.81% of the length of the cable (4.60m). The magneto-rheological damper is attached at 4.81% of the cable (7.88m), with a maximum force of 45kN at a current of 3A, a residual force at zero tension of 2kN and a relatively low viscous coefficient in passive mode of only 4.99 kN/s.

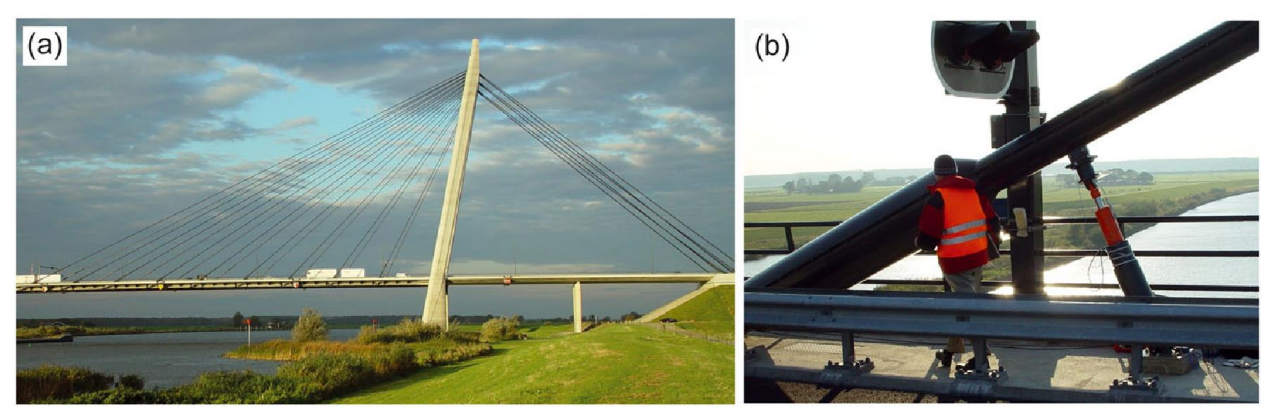


Figure 32 – Eiland bridge, Kampen-Netherlands

Considering all the above stated, the following principles must be taken into account when designing a magneto-rheological damper:

- The force generated by the device must be able to provide damping regardless of the frequency of oscillations, due to the very wide range of phenomena that can induce vibrations in the stays
- The number of sensors and the complexity of the control system must be as small as possible to increase the robustness of the apparatus
- The control force variation must not contain components with a very high frequency because it cannot be tracked by the instrument due to the extremely small bandwidth
- The optimal force in the device must be generated with small errors, based on a mathematical model that can record and adapt this value in real time

One of the most important applications of this damping system is in the case of the Sutong Bridge, with stays of lengths between 154m and 543m. It was decided to mitigate vibrations with passive viscous dampers at the cables numbers numbers 10 (L=228m, T=1.785s) to 28 (L=472m, T=3.571s), and for the longest 6 stays, respectively numbers 29 (L =483m, T= 3.584s) to 34 (L=543m, T=4.002s) with magneto-rheological dampers.



Figure 33 - Dampers on Sutong Bridge, China

The devices were installed perpendicular to the cables in their vertical plane, 3.50m above the deck. The anchors are located 1.30m below the deck level, thus resulting in a relative position of the devices of approximately 2.30% of the cable length. Each stay has an individual sensor

mounted that transmits the data to a central control unit, positioned inside the superstructure, which can control all 12 dampers. As an additional measure, each device is connected external batteries, capable of ensuring its operation for at least 48 hours in the event of a power failure.

Similar systems were used in the cases of the Franjo Tudjman bridges near Dubrovnik, Croatia, or the Alamillo bridge in Seville, Spain, where it was implemented as a measure of rehabilitation.

The system was tested on a scale model in 2007, on a cable similar to the one on the Sutong Bridge, with a length of 228m.

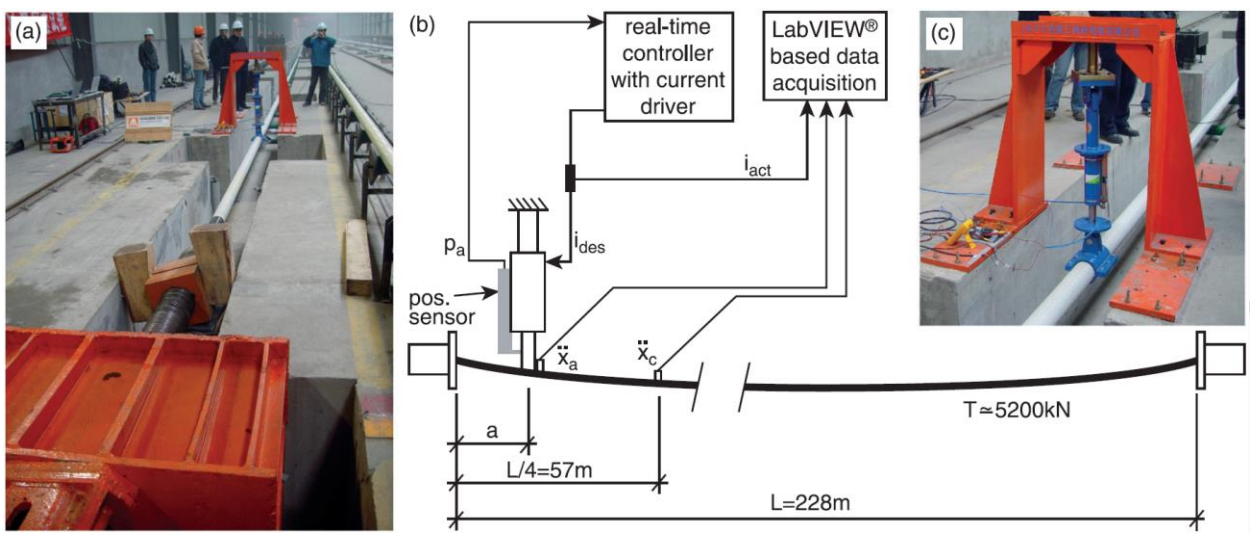


Figure 34 – Testing of magneto-rheological dampers, China

The test results showed that both the calculation assumptions and the control systems worked correctly, registering a 7.5% damping. The influence of the real stiffness of the cable, which turned out to be lower than the theoretical values, and the rotation in the anchorages, which turned out to be higher than had been considered in the calculation assumptions, were also highlighted.

The most recent use of these systems was at the Russky Bridge in Russia. Similar to the Sutong Bridge, passive viscous dampers were installed on the shorter cables numbered from 1 to 16, and on the longer spans from 17 (L=483m, T=3.571s, a/L=2.6%) to 21 (L=580m, T=4.165s, a/L=2.3%) magneto-rheological dampers were installed. Unlike the Sutong bridge, in order to reduce power consumption, in this case each device had separate control units and accelerometer sensors mounted directly on the cables at approximately 28.00m from the deck. Also, the devices used in this bridge include 2 dampers in each direction, in order to mitigate vibrations in the horizontal plane as well. The biggest innovation in this system, however, is that the magneto-rheological dampers also have temperature sensors and can make the necessary corrections to ensure optimal damping between -40°C and +60°C.

III. CASE STUDY: DYNAMIC RESPONSE OF A CABLE WITH EXTERNAL VIBRATION DAMPING SYSTEMS

III.1. Objectives

The case study aims to analyze the dynamic response of a cable during large amplitude vibrations. To achieve this, it's behavior will be analyzed in two particular situations:

- the response of the cable at resonance under an external excitation that will produce vibrations in it and even lead to resonance phenomena with high amplitudes and stresses
- cable response to free vibration with time tracking of oscillation damping

Another goal is to establish the influence of different types of external dampers on cable deformation, anchorage forces, system damping and energy dissipated.

Parameters to be monitored:

- the maximum and minimum displacements of the midpoint of the cable in order to establish the maximum amplitude during forced vibration
- the maximum and minimum reactions in the anchors to establish the stress difference for fatigue checks
- total cable damping (with or without energy dissipating devices) to determine the overall stability of the cable under vibrations
- the energy dissipated by the vibration damping devices in order to estimate the efficiency of each device

III.2. The calculation model

For this study, it was necesary to simulate the cable responses of cable-stayed bridge under dynamic wind actions using the finite element method. A 300m-long isolated cable stay with the following physical-mechanical characteristics was studied:

- > Stay cross section
 - 37 T15S strands with a total area of 5550 mm² (37×150 mm²)
 - Protective sheath made of high-density polyethylene with an outer diameter of 155mm and a thickness of 6mm
- Material oțel de înaltă rezistență Greutate volumică γ =78.50 kN/m³
 - Efort unitar de curgere f_t=1770 N/mm²
 - Modul de elasticitate E_o=195 Gpa
- Material high resistance steel Volumetric weight γ =78.50 kN/m³

Unit yield stress f_t=1770 N/mm²

Modulus of elasticity E₀=195 Gpa

- ➤ Overall characteristics Cable lengths: 50m, 100m, 200m, 400m
 - weight per meter: 500N/m

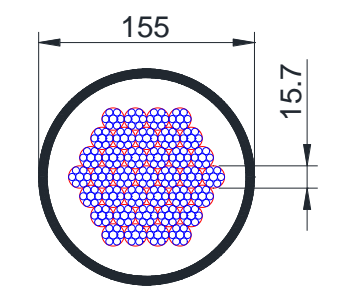


Figure 35 - Stay cross section

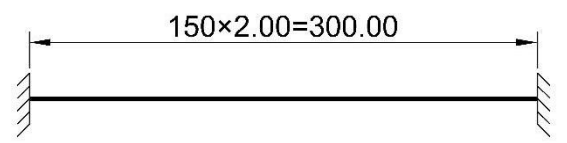


Figure 36 – Free cable calculation model

Several computational models were made for each isolated stay. The cables were modeled with 150 bar-type elements, supported at the ends. For end supports, the blocking of movements in all directions was considered. A fine level of discretization was constructed, non-linear-time history type of analysis was considered and a very correct introducing the physical-geometrical characteristics was done, in order to obtain more accurate results. The adopted finite elements have both axial stiffness and shear force, bending and torsion (summing the stiffnesses the 37 individual strands). It was assumed that the unit stress in the stays corresponded to the Service Limit State and did not exceed 45% of the yield strength.

It is well known that the tension inside the cables strongly influences their dynamic response. They become more susceptible to vibration as the internal tension decreases. In this regard, only the self-weight of the rope and a prestressing force were considered as permanent actions, and an external force from the wind, with variation in time, acting in the transverse direction of the cable.

Since the action of the wind has an unpredictable character, and its variation over time can manifest itself in different forms, a sinusoidal function was chosen as the law of variation, with a period that corresponds to the fundamental period of vibration of the considered system, all this to ensure the appearance of resonance. The maximum value of this force was considered (according to Electives 1 and 2, of the Ph.D.) to be one-tenth of its own weight per linear meter.

$$p(t) = \left(\frac{t \cdot \pi}{T}\right)$$
, where *T* is the period of the fundamental mode of vibration

III.3. Validation of the calculation model

An experimental study carried out by the University of Windsor entitled "Experimental Study on Bridge Cable Vibration Mitigation Using External Viscous Damper" was used to validate the calculation model, the considered assumptions and the calculation parameters. It involves, among other things, making a scale model for an isolated cable and analyzing its dynamic response under free vibrations.

The experiment was carried out on a high-strength steel cable with a length of 9.33m, with an outer diameter of 4.65mm and a weight of 0.092 kg/m. Its area is 11.90mm², and the moment of inertia is 15.8mm⁴. To artificially increase the period of the first natural vibration mode, 20 additional masses of 50g each were added at a constant distance along the length of the cable.

The cable was anchored at one end to a force sensor (to determine tension) and at the other to a manual hydraulic press (to induce an initial stress state). To measure the displacements of the cable, an accelerometer was installed in the middle of it, perfectly perpendicular to the cable.

The tension induced in the cable was 3.2kN, resulting in a theoretical vibration period of 0.146s. To induce vibrations in the cables, an 8kg weight was attached to its middle with a thread. By instantaneously cutting the connecting wire, the cable, which is in a deformed position, will try to suddenly return to its original position, thus resulting in free vibration.





Experimental data:

Cable length – 9.33m Cable diameter – 4.65mm Weight -0.092 kg/m

Moment of inertia: 15.8mm⁴ Prestressing force: 3.2 kN

Additional weights: 20 pieces 50g each

Final weight per meter: 0.2 kg/m



Figure 37 – Scale model

A computational model with finite elements was done for comparison. To shape the cable, 29 bar-type elements anchored at the ends by perfect fits were used. Nonlinear analyzes with Pdelta effects and large displacements were performed in the order presented below, taking the state of stresses and strains from one stage to another:

- 1. Static loading with the cable's own weight
- 2. Static loading with a prestressing force of 3.2kN
- 3. Dynamic Time history analysis with direct integration includes loading with 8kg weight and the dynamic response of the cable after its removal over a 25s time period

In the case of the dynamic analysis, the key to obtaining results as close as possible to reality is the correct determination of the mass damping and stiffness coefficients, according to Rayleigh damping model. They were estimated to obtain a damping corresponding to the first vibration mode of 1%, and for the third mode of 0.5%.

The comparisons between the experimental and the theoretical model were made by analyzing the deformed shape over time for the point in the middle of the cable, the maximum amplitudes for certain oscillation cycles, respectively the estimated damping.

Tabelul 2 – Comparison of the critical damping percentages obtained

Considered	Calculated	Measured	Differences
cycles	%	%	%
1 si 2	1.45%	1.76%	17.37%
1 si 4	1.75%	1.81%	3.57%
1 si 6	2.16%	2.02%	-6.75%
1 si 9	2.69%	2.07%	-30.10%

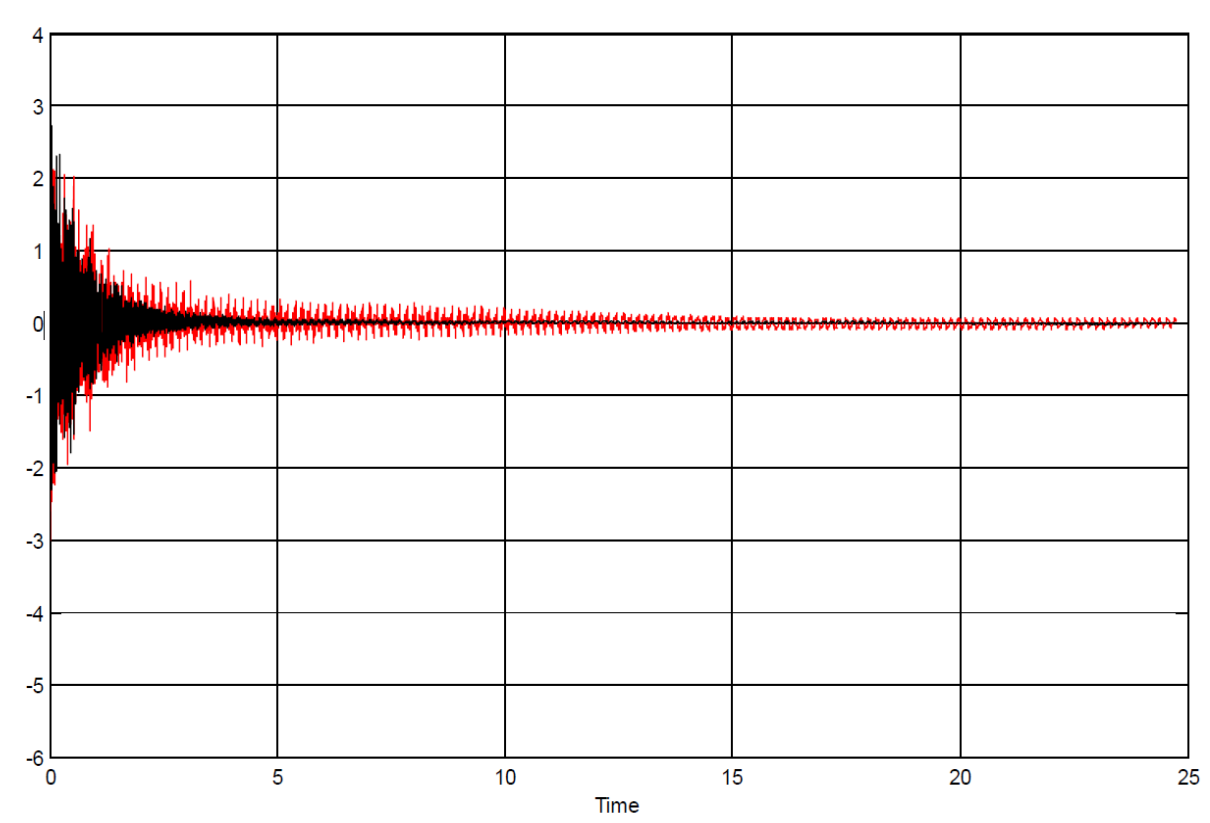


Figure 38 – Time variation of mid-cable amplitudes on the experimental model

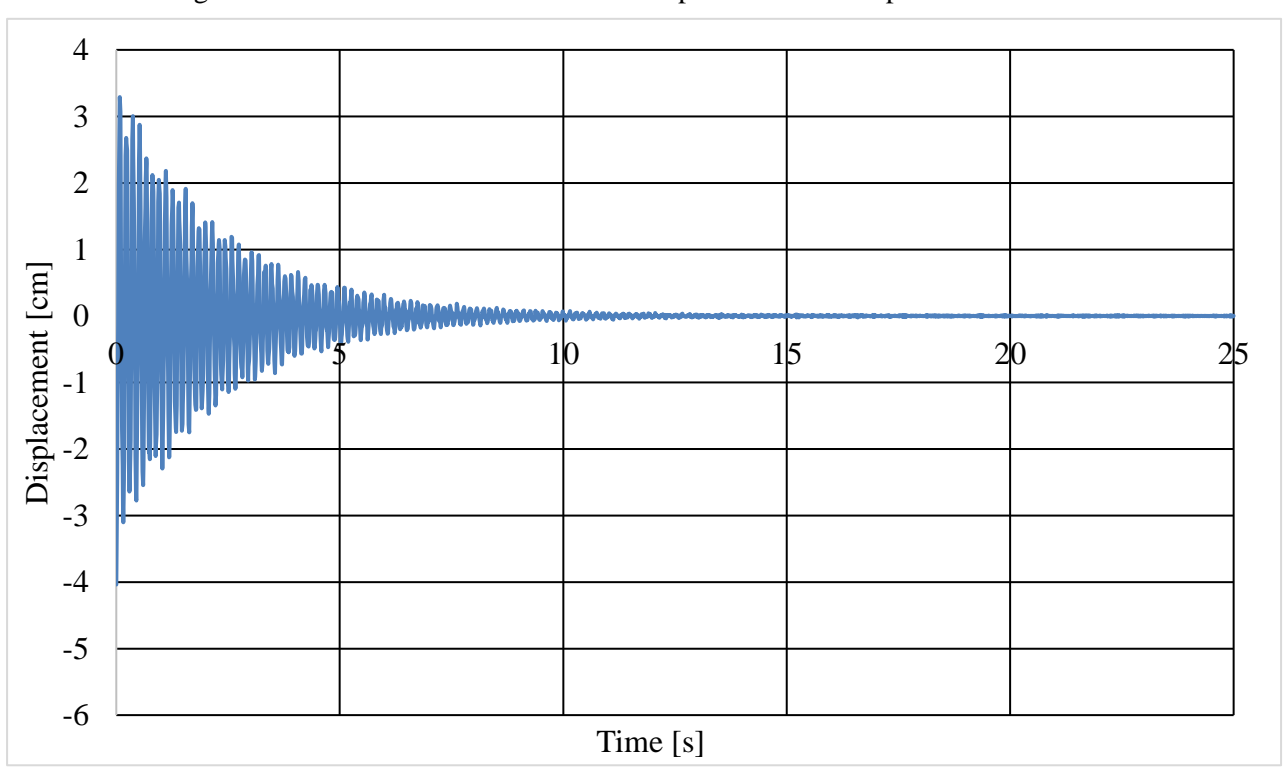


Figure 39 - Time variation of the amplitudes in the middle of the cable on the theoretical model

Considered	Calculated	Measured	Differences
cycles	[cm]	[cm]	%
1	3.495	3.516	0.59%
2	2.784	2.793	0.30%
4	2.351	2.082	-12.95%
6	1.857	1.388	-33.81%

Regarding the damping, as it can be seen both in the comparative tables and in the time variation of the displacements, greater differences are found between the models towards the end of the analysis. Taking into account the inaccuracy of the calculation method, the resulting differences are within acceptable limits.

As for the displacements, they are smaller in the calculation model which is more rigid. Although the allure is preserved, there is a difference in amplitudes of about 0.2cm from the beginning, a difference that is preserved until the end.

The shape of the variation of the amplitudes over time is almost identical, with small differences in the decay of the damping with time. In the experimental model, the damping decreases faster, and the cable maintains amplitudes until the end of the recordings. In the theoretical model this decrease is slower, leading to a better damping of small amplitude vibrations that almost die out after about 15s of the analysis.

Taking into account all the differences stated above, between the calculated and the recorded dynamic behavior of the cable, it can be concluded that the differences are small, below the acceptable threshold. The proposed method of approach by numerical modeling can therefore be applied to other situations, such as those presented below.

III.4. Free cable

In order to establish a baseline for comparison between different vibration damping systems, an analysis was initially performed on the cable without any attached device. The following table shows the maximum and minimum values of the studied parameters:

ruser i maximum minimum parameter varies for the free custe							
Displaement in the middle			Bending m	Damping			
Max	Min	Amplitude	Max	Min	Amplitude	%	
[mm]	[mm]	[mm]	$[kN \times m]$	$[kN \times m]$	$[kN \times m]$	70	
3068 24	-6194 47	9262 71	23 64	-73 20	96.83	0.315%	

Tabel 1 –Maximum/minimum parameter values for the free cable

For a better understanding of the dynamic response of the cable, graphs are presented below with the time variation of the displacement of the point in the middle of the cable, respectively of the bending moment in the anchorage.

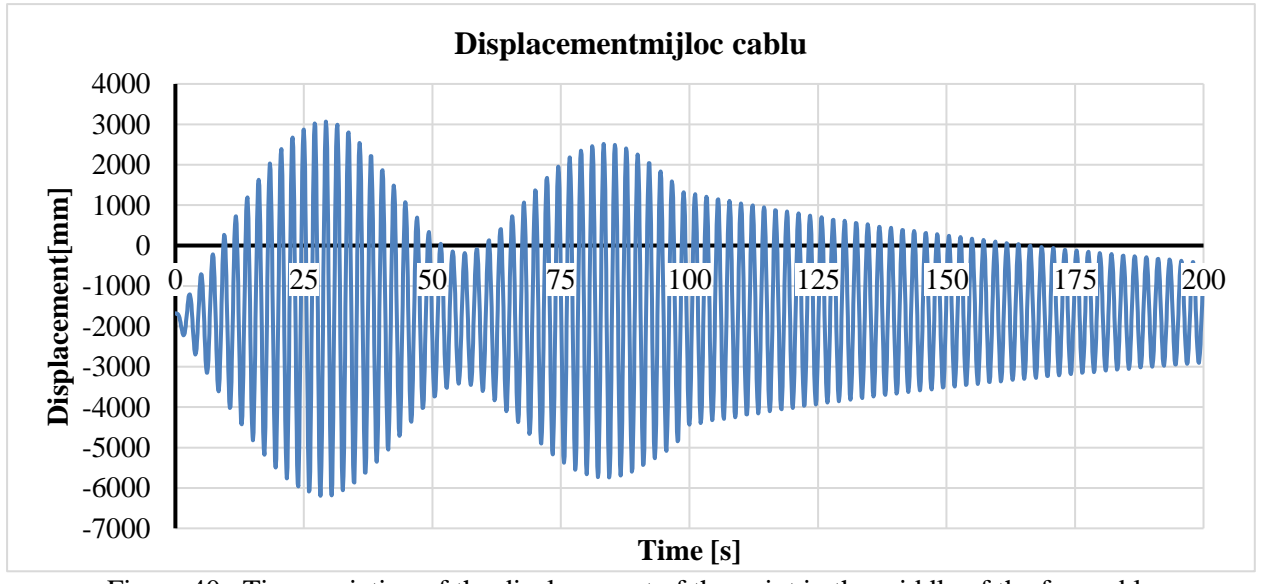


Figure 40 – Time variation of the displacement of the point in the middle of the free cable

Regarding the displacements, it can be seen that the oscillations are symmetrical with respect to a horizontal line that does not pass through the origin, but through the ordinate of - 1680mm, corresponding to the displacement due to the cable's own weight. The oscillations are

cyclic with a constant period of 2.10s, equal to the period of the first natural mode of vibration of the cable.

One can clearly observe the resonance phenomenon that leads to increasing the maximum amplitudes from one cycle to another. Analyzing the peaks of the oscillation amplitudes, it can be seen in the zones under forced vibrations that they increase and decrease after 2 cycles with a period of approximately 58.40s. The first cycle has larger amplitudes most likely due to higher inertial forces resulting from starting from rest. The second cycle keeps the allure of the first, but with smaller amplitudes by about 20%. If the external excitation would have continued to act on the cable, other cycles with the same variation, amplitudes and period as the second would be formed.

A mitigation of vibrations can be observed in the free vibration area. The envelope of the amplitudes describes an asymptotic variation law that tends to the horizontal around the value of the amplitudes of about 2000mm. This means a decrease in the internal damping in the cable depending on the magnitude of the cable deformations, from the maximum value of 0.315% to a value of only 0.16%.

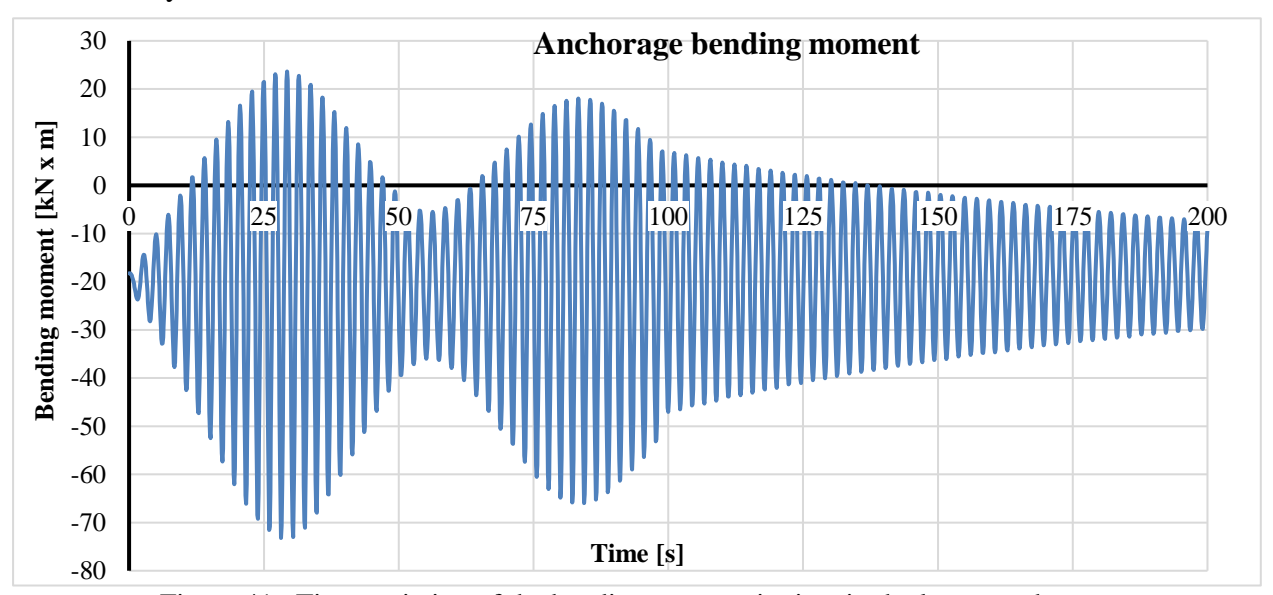


Figure 41 –Time variation of the bending moment in time in the lower anchorage

By analyzing the variation of the bending moment in the anchorages, the same pattern can be found as in the case of displacements, with oscillations around a reference line of $18 \text{ kN} \times \text{m}$, 2 cycles of amplitude variation during the period of forced vibrations and an asymptotic attenuation of oscillations in the area free vibrations. However, there are small differences in the shape of the cycles, which are slightly sharper.

III.5. Tuned mass dampers

In this analysis, the influence of the attachment of certain masses on the beam and its dynamic response were studied. As a solution, 2 tuned masses were adopted, each with a mass of 0.50 tons, equivalent to the weight of 10 meters of cable. The goal of the analysis is not to increase the damping of the system, but to shift the periods of the eigenmodes of vibration so that excesively large amplitudes are no longer reached in the oscillation cycles.

Next, the variation in time of the displacement of the point in the middle of the cable, respectively of the bending moment in the anchors, are presented.

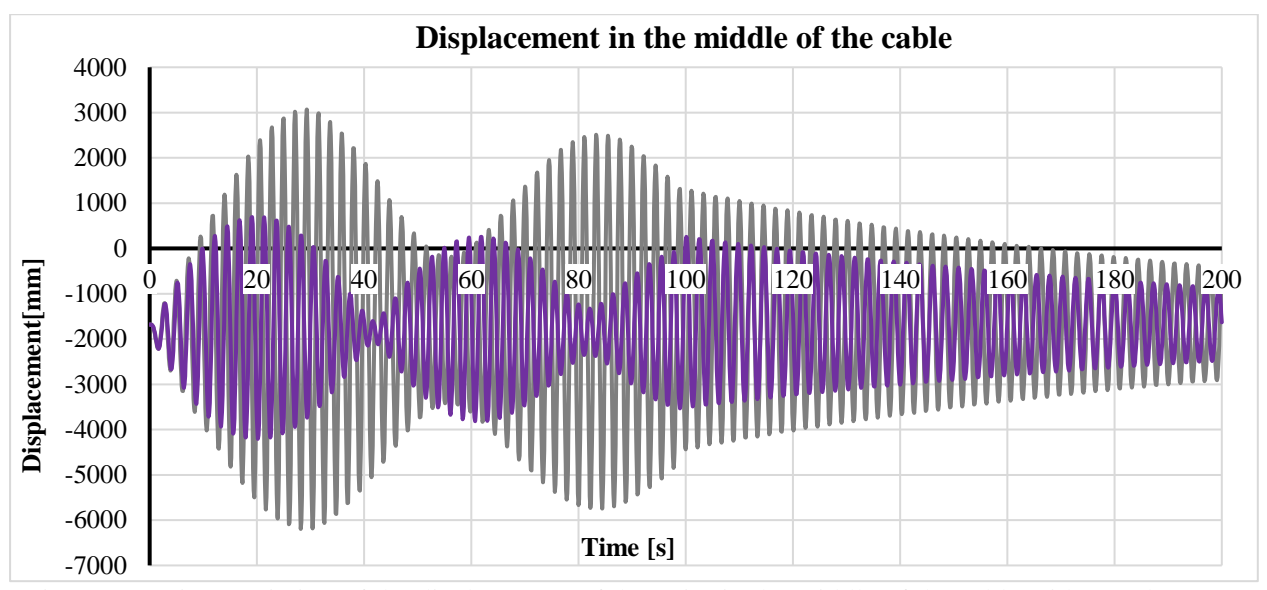


Figure 42 – Time variation of the displacement of the point in the middle of the cable with tuned masses

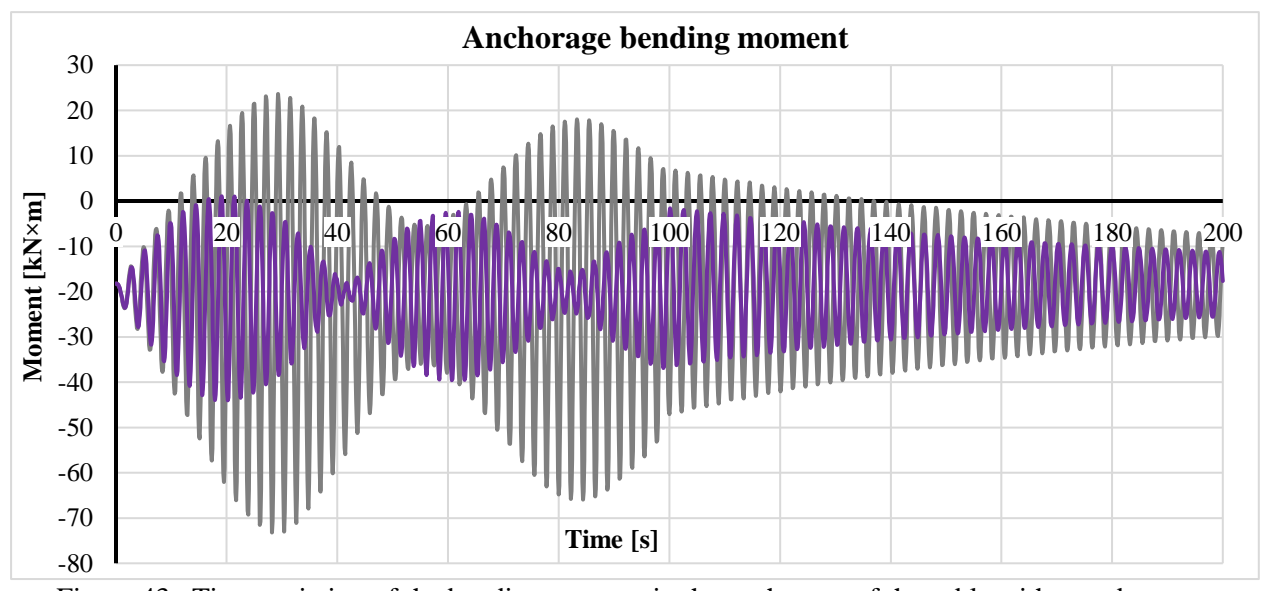


Figure 43 – Time variation of the bending moment in the anchorage of the cable with tuned masses

Tabel 2 – Maximum/minimum parameter values for the cable with tuned masses

Displacement in the middle of the cable			Anchor	Damping		
Max	Min	Amplitude	Max	Min	Amplitude	%
[mm]	[mm]	[mm]	$[kN \times m]$	$[kN \times m]$	$[kN \times m]$	90
692.53	-4204.96	4897.50	1.04	-44.01	45.06	0.28%

By analyzing the above, it can be seen that both the amplitudes of the displacements and those of the bending moment are much smaller during the period of forced vibrations. The maximum amplitude curves describe shorter cycles with half the initial values. Although the total mass of the system increased, the period of these cycles decreased to about 40s. In the area of free vibrations, a more unfavorable response of the stay is observed, the resulting internal damping actually decreasing. For this reason, the cycles tend to be similar towards the end of the analysis.

Although at first sight it would seem that the system is extremely efficient, it should also be taken into account that the change in the natural period of the cable led to smaller resonance phenomena, the period of the excitation function being further away from the critical one and this could not be the case for other excitation forces.

III.6. Cross ties

In this analysis, the influence of attaching cross ties between the stays on their dynamic response was studied. For the study, in addition to the initial cable, one parallel to it at a distance of 10.00m from it was modeled, with a length of 280.00m, and a cross tie connected between them at a distance of 60.00m from the opposite end to the studied anchorage were used. The purpose of the analysis is to study how the 2 cables interact with each other and modify each other's dynamic response.

Next, the variation over time of the displacement of the point in the middle of the cable, respectively of the bending moment in the anchors, is presented.

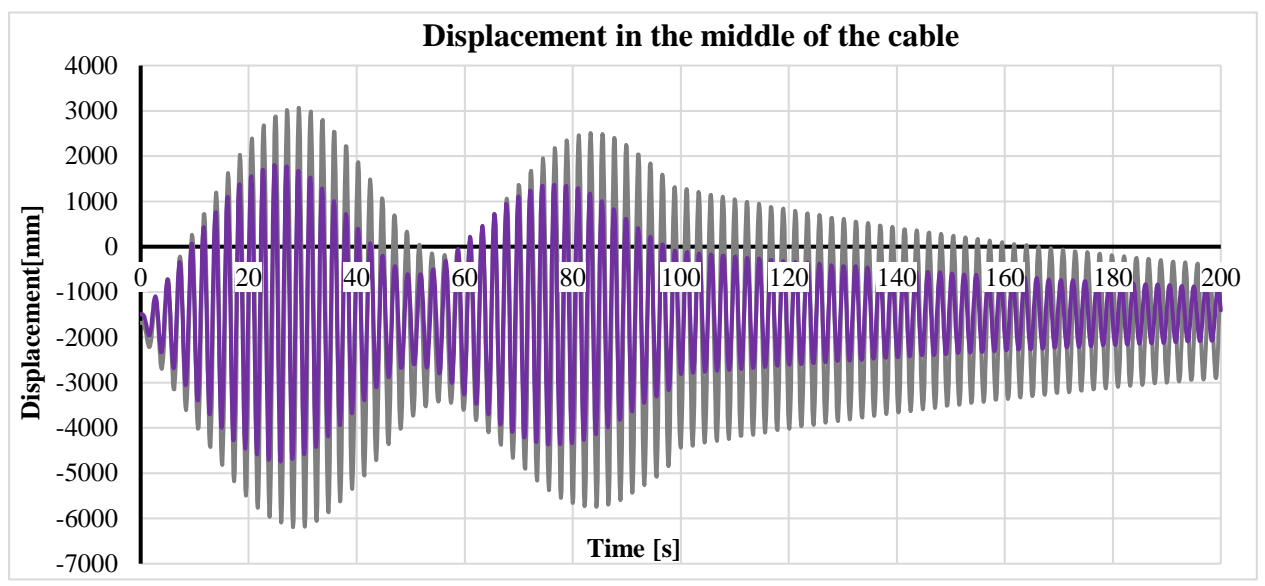


Figure 44 – Time variation of the displacement of the midpoint of the cable with cross ties

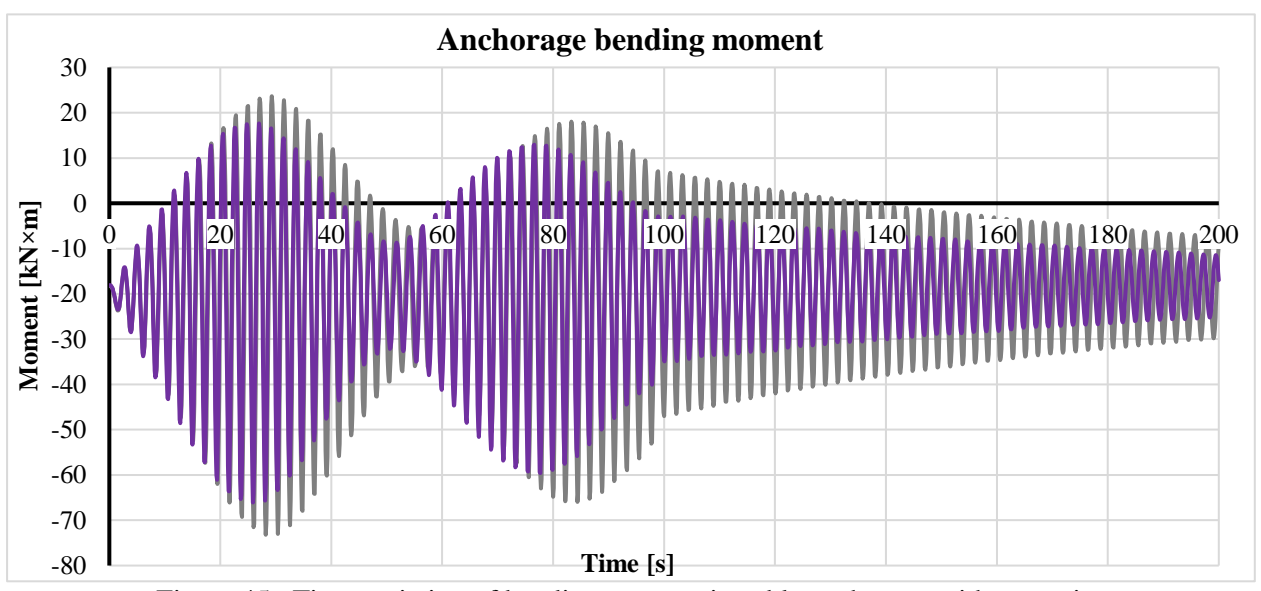


Figure 45 – Time variation of bending moment in cable anchorage with cross ties

Tabel 3 – Maximum/minimum values of the parameters for the cable with cross ties

Displcement in the middle of the cable			Bending m	Damping		
Max	Min	Amplitude	Max	Min	Amplitude	%
[mm]	[mm]	[mm]	$[kN \times m]$	$[kN \times m]$	$[kN \times m]$, ,
1803.88	-4746.09	6549.97	17.62	-66.07	83.70	0.31

The cables were considered to be adjacent and thus have similar dynamic characteristics, yet different enough to influence each other and not vibrate coupled.

Analyzing the data presented previously, it is observed that in the area of forced vibrations, the influence on the displacement is greater than that on the stresses in the anchorage, which are similar to the results from the analysis of the free cable. The peak amplitudes appear to follow the rise/fall slopes of the free cable cycles, but with lower values and reduced period to about 50s.

In the free vibration area, the cycles appear to be at a lower level than the reference values but this is probably due to coincidence. The external excitation stops acting at a moment of much smaller amplitudes compared to the case of the free stay, due to the shortening of the cycles. Moreover, the mitigation is also inferior to the original system in this case.

III.7. Viscous dampers

This analysis studies the influence of attaching a viscous damper to a cable has on its dynamic response. The viscous dampers, like the elastomeric ones, were installed at one end of the stay, at a distance of 4.00m from it (1.13% of its length). As for the calculation parameters, an elastic stiffness of the fluid of k=10000 kN/m, a speed exponent $\alpha=0.8$ was considered, and for the viscous coefficient c a parametric study was made with its variation from 0 to 1500 kN x s/m. Although there are calculation methods for determining the optimal viscous coefficient prescribed in literature for each vibration mode separately, it is considered that a single vibration mode is not enough, the first 4-5 having a significant impact.

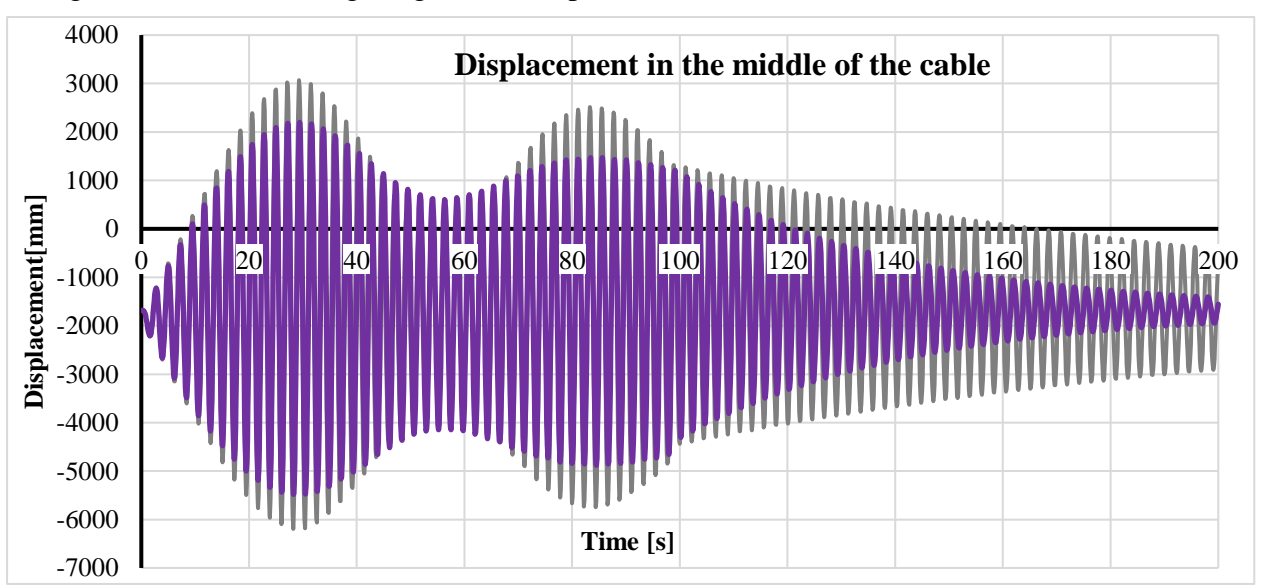


Figure 46 – Time variation of midpoint displacement of viscous damper cable

By studying the displacement over time of the point in the middle of the cable, small attenuations of the amplitudes during the forced vibrations and a much sharper decrease of the oscillations in the area of free vibrations can be observed. The allure is similar to that of the free cable, but with a lower level of amplitudes. Towards the end of the analysis, the amplitudes drop even below the level of 350mm. The following table shows the maximum and minimum values of the displacement of the middle of the cable, as well as the oscillation amplitudes, all depending on the chosen viscous coefficients.

c			Displacemen	t in the middle of the cable		
[kN/s×m]	Max [mm]	Min [mm]	Amplitude [mm]	9500		
0	3068.24	-6194.47	9262.71	9250		
50	2774.05	-5948.94	8722.98	## 9000 \$8750 ## 8500 ## 8250		
100	2534.01	-5759.51	8293.52	8500 Line 8500		
200	2198.46	-5480.61	7679.07	Example 19 Example 19 Exam		
220	2161.46	-5452.02	7613.48			
250	2118.66	-5419.06	7537.72	7750		
300	2072.01	-5381.02	7453.03	mm 7750 xx 7500 7350		
350	2052.83	-5355.72	7408.55	≥ 7250		
400	2044.03	-5343.21	7387.24	7000		
500	2092.23	-5387.81	7480.04	0 200 300 300 500 600 600 600 100 100 200 500		
600	2132.80	-5424.57	7557.37	Viscous coefficient[kN x s / m]		
1000	2226.50	-5510.75	7737.25	Figure 47 – Variation of maximum amplitude over		
1500	2273.73	-5551.34	7825.07	viscous coefficient of the device		

By analyzing the results presented above, it can be seen that the optimal value of the viscous coefficient for the smallest amplitudes is around the value of $400 \text{ kN} \times \text{s/m}$, which corresponds to a maximum amplitude of 7387 mm.

Next, there is a similar comparison will regarding the bending moment in the stays anchorage.

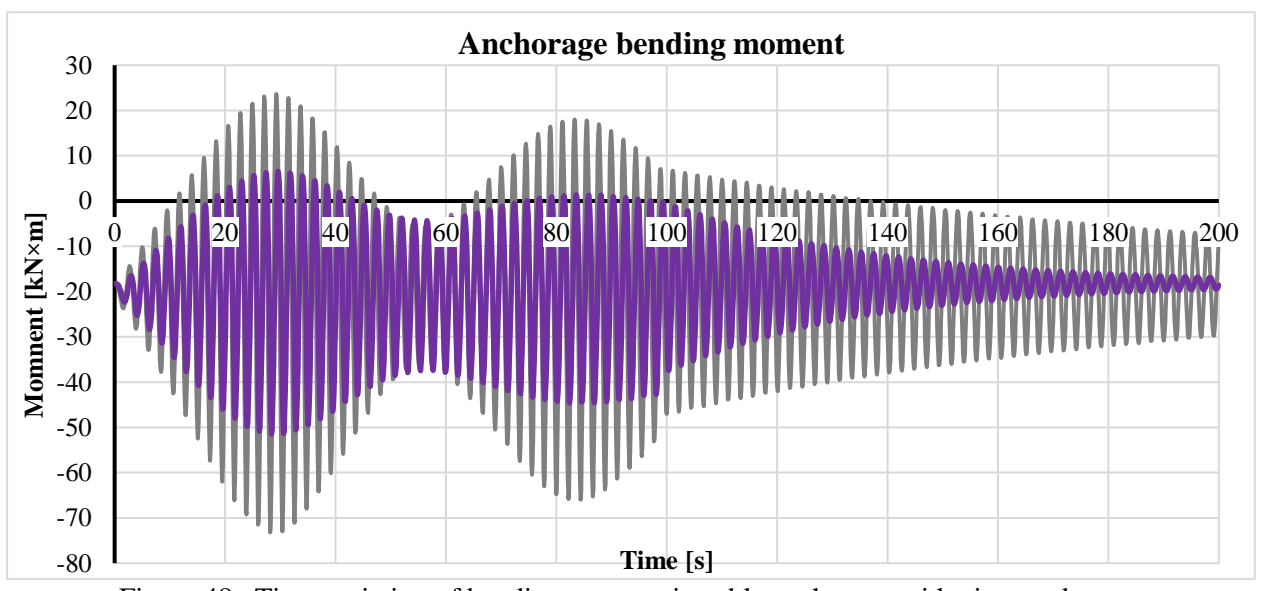


Figure 48 – Time variation of bending moment in cable anchorage with viscous damper

c	Bending moment in anchorage						
[kN/s×m]	Max	Min	Amplitude	110.00			
[11 (/ 5/ 111]	$[kN \times m]$	$[kN \times m]$	$[kN \times m]$	100.00			
0	23.64	-73.20	96.83	90.00			
50	19.69	-68.44	88.13	80.00			
100	15.10	-62.24	77.34	70.00			
200	6.57	-51.48	58.05	T 60.00			
220	5.10	-49.68	54.78	00.00 50.00 40.00			
250	3.10	-47.28	50.38				
300	0.42	-43.95	44.37	30.00 20.00 10.00			
350	-1.73	-41.31	39.58	1 0.00			
400	-3.51	-39.21	35.70	0.00			
500	-6.22	-36.13	29.92	0 100 3300 3300 500 600 600 600 600 100 100 100 500			
600	-8.17	-34.00	25.84	Viscous coefficient[kN x s / m]			
1000	-12.15	-30.02	17.87	Figure 49 – The variation of the bending moment			
1500	-14.02	-28.59	14.56	according to the viscosity of the device			

From the above, it would appear that the anchorage moment decreases with the increase of the viscous coefficient. This is because the damper exerts an ever-increasing force on the cable, reducing its rotations at the ends. The benefits brought by this for the anchorage, however, have a negative impact on the cable. From around $600 \text{ kN} \times \text{s/m}$ of the "c" parameter, forces over 120 kN start to appear in the piston head, which can degrade the cables sheath, thus limiting the possibility of increasing the viscosity above this threshold. However, for the value under discussion a sectional stress difference of $25.84 \text{ kN} \times \text{m}$ was obtained, well below the maximum value of $96.83 \text{ kN} \times \text{m}$ corresponding to the free cable.

The following tables and graphs show the energy dissipated by the device at different stages of the analysis and the damping (expressed as a percentage of the critical damping) of the whole system.

c	Dis	Damping		
[kN/s×m]	Forced vibration [kJ]	Free vibration [kJ]	Total [kJ]	%
0	0.00	0.00	0.00	0.315%
50	376.35	108.28	484.63	0.543%
100	640.02	143.46	783.48	0.737%
200	803.97	141.18	945.16	0.881%
220	798.63	137.25	935.88	0.881%
250	778.53	131.64	910.17	0.869%
300	727.15	121.78	848.93	0.807%
350	667.86	112.21	780.07	0.762%
400	609.65	103.33	712.98	0.725%
500	507.76	87.90	595.66	0.678%
600	427.94	75.29	503.24	0.618%
1000	248.42	44.23	292.64	0.444%
1500	155.43	27.17	182.60	0.386%

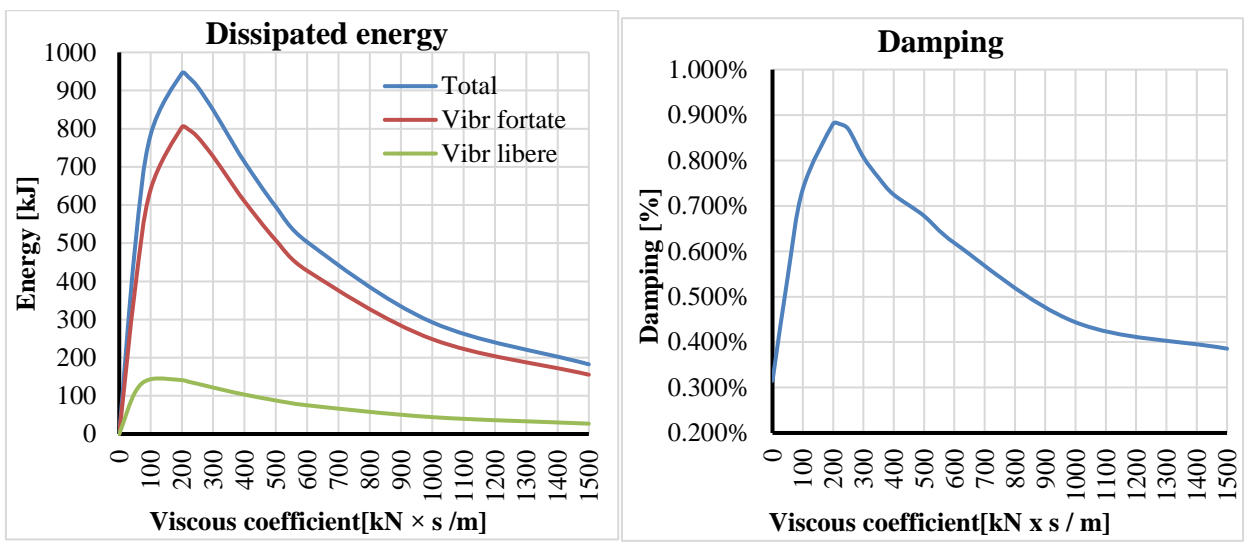


Figure 50 – The energy dissipated by the device and the damping according to its viscosity

By analyzing the data presented above, one obvious conclusion can be drawn, namely that the damping of the system is directly proportional to the energy dissipated by the damper, even if certain values of the viscous coefficient gave better results during forced vibrations and vice versa for others.

The optimal viscous coefficient for energy dissipation is different for forced versus free vibrations, and the slope of the energy dissipated when changing it differs in the 2 analyses. It is found, however, that the optimal value is around 220 kN \times s/m, a value corresponding to the maximum damping of the system.

Through a simplified calculation, the optimal damping coefficients for the first 5 cable vibration modes were identified, as follows:

Modul	1	2	3	4	5
C [kN×s/m]	308.5	154.25	102.8	77.1	61.7

As can be seen, the optimal value for this parameter is somewhere between the optimal one for the first and second modes. This is due to the influence that the higher modes also have on the behavior of the cable.

Regarding the allure of the efficiency of the damping system related to the viscosity of the device, it can be seen that, starting from a value of zero until reaching the optimal value, there is an interval of steep increases, and after overcoming it, the decrease in efficiency is much smoother, almost asymptotic.

To better demonstrate the device's operating principles, the force-displacement hysteresis curve of the damper is presented below.

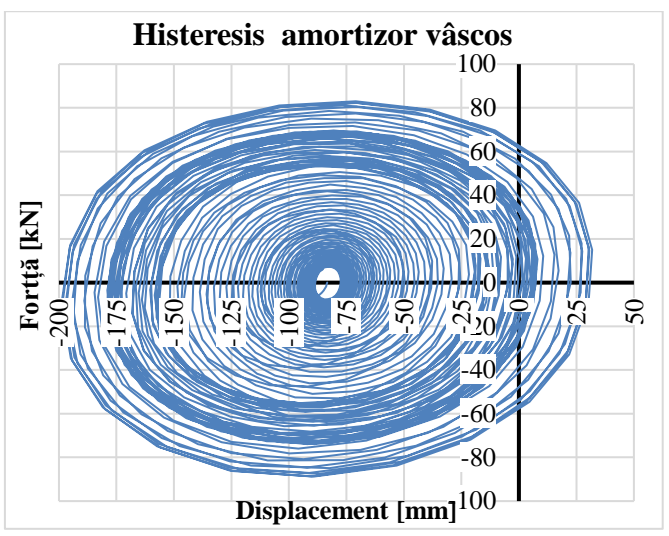


Figure 51 – Viscous damper force-displacement curve

The curve described by the device is specific to viscous dampers. Due to the exponent α =0.8, concentric ellipses can be observed with the center in the value of 0 of the force and -83mm of the device, corresponding to the rest state of the cable. Obviously, the efficiency of the device is higher with increasing displacements, but unlike other energy dissipation mechanisms, it generates manual work even at a low level of amplitudes.

III.8. Elastomeric dampers

In this analysis, the influence of attaching an elastomeric damper to the cable has on its dynamic response was studied. The elastomeric dampers were installed at one end of the stay, at a distance of 4.00m from it (1.13% of the length). For a better understanding of their influence on the dynamic response of the cables, a parametric study was carried out with the variation of the elastic limit between 10kN and 60kN, respectively the shear stiffness of the elastomer of 750kN, 1500kN, 3000kN and 5000kN. The variation of the ratio between elastic and post-elastic stiffness is a material characteristic and was not studied lower values of this parameter always better results.

Below are presented the variations of the deformation of the point in the middle of the cable, respectively of the bending moment difference in the anchorage, depending on the varied parameters:

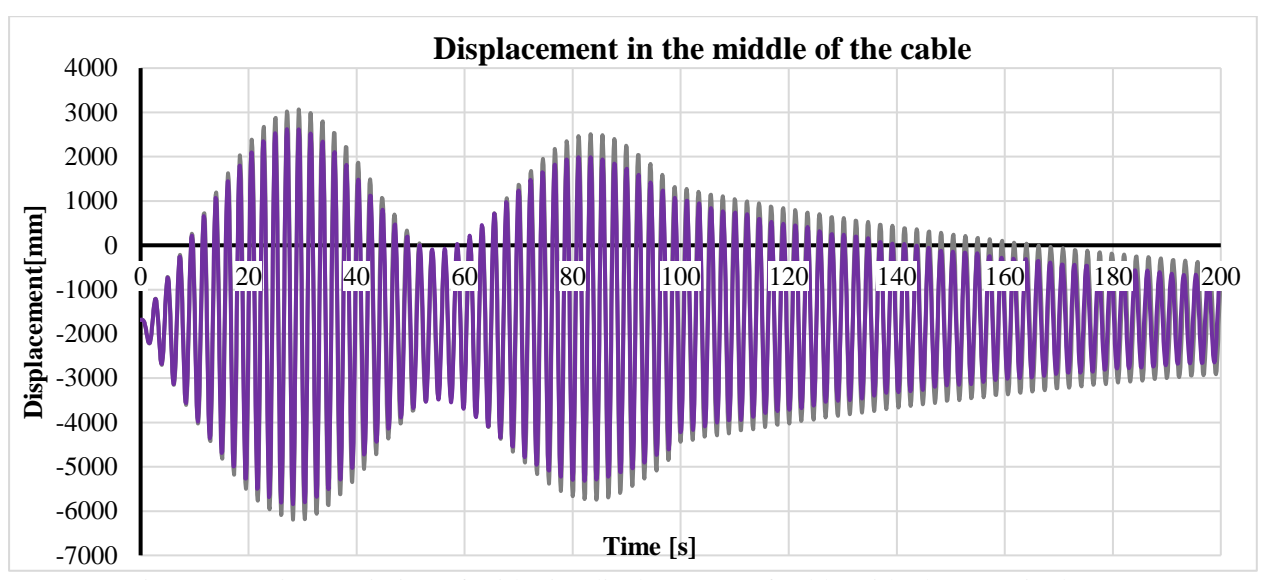


Figure 52 – Time variation of midpoint displacement of cable with elastomeric damper

Stiffnes s	\mathbf{f}_{el}	Displacement in the middle of the cable							
kN/m	[kN]	Max [mm]	Min [mm]	Amplitude [mm]					
	15	2797.89	-5979.69	8777.59	8900				
k=750	20	2762.05	-5952.16	8714.21	8800				
	25	2734.61	-5933.23	8667.84	8700				
	30	2715.59	-5921.33	8636.92					
	10	2592.54	-5814.52	8407.06	8600				
k=1500	20	2681.31	-5892.35	8573.66	9 8500				
	30	2622.15	-5844.29	8466.44	iller 8400				
	40	2592.54	-5814.52	8407.06	E 2000				
	60	2581.11	-5794.48	8375.59	8600 8500 8500 8400 8200 k=1500 k=3000				
	20	2601.37	-5819.58	8420.95	8200 k=1500				
	25	2574.32	-5796.03	8370.35	** 8100				
k=3000	30	2550.24	-5774.35	8324.59	8000 — k=5000				
	35	2529.33	-5754.87	8284.19	\$ \$ \$ \$ \$ \$ \$ \$ \$ \$ \$ \$ \$ \$ \$ \$ \$ \$ \$				
	40	2511.68	-5738.14	8249.82	Limită elasticitate [kN]				
	30	2496.14	-5719.45	8215.60	Figure 53 – Variation of the displacement according to				
k=5000	35	2477.85	-5705.16	8183.00	the characteristics of the device				
V-2000	40	2461.57	-5692.84	8154.41					
	45	2447.27	-5682.54	8129.80					

It can be seen that the smallest displacements correspond to more stiffness of the cables and larger elastic limits. The maximum values of the displacement amplitudes decrease to approximately $8650 \, \text{mm}$, for stiffness k=750 kN/m, $8375 \, \text{mm}$ for k=1500kN/m, $8200 \, \text{mm}$ for k=3000kN/m, respectively $8085 \, \text{mm}$ for k=5000kN/m.

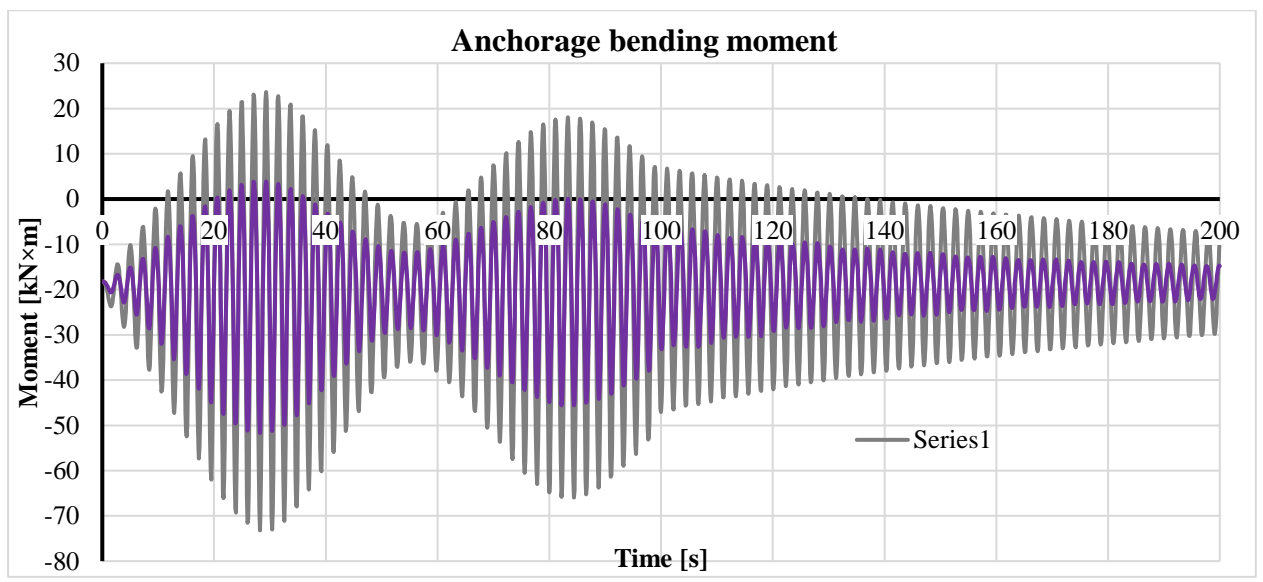


Figure 54 – Time variation of bending moment in cable anchorage with elastomeric damper

Stiff ness	$\mathbf{f}_{ ext{el}}$			Bending me	oment in the anchorage
kN/m	[kN]	$\begin{array}{c} \text{Max} \\ [kN \times m] \end{array}$	Min [kN × m]	Amplitud e $[kN \times m]$	75
	15	11.65	-60.31	71.961	75
k=75	20	10.66	-59.19	69.85	70
0	25	9.75	-58.17	67.91	E 65
	30	8.87	-57.23	66.11	$\mathbf{\ddot{Z}}$ 60
	10	2.47	-50.08	52.55	Sep 55
1 15	20	5.48	-53.49	58.98	mig. 50
k=15 00	30	3.90	-51.68	55.57	du
00	40	2.47	-50.08	52.55	a 45
	60	0.04	-47.26	47.30	Waximum amplitudes [KN 60 55 55 55 45] Waximum 40 40 40 40 40 40 40 40 40 40 40 40 40
	20	-0.89	-46.11	45.22	id 35
1 20	25	-1.44	-45.44	44.00	30
k=30 00	30	-1.99	-44.76	42.77	25
00	35	-2.53	-44.11	41.58	10 10 15 20 20 25 25 30
	40	-3.05	-43.47	40.42	Elas
	30	-6.35	-39.39	33.03	Figure 55 –Bending function of the de
k=50	35	-6.71	-38.90	32.18	runction of the de
00	40	-7.09	-38.43	31.34	
	45	-7.47	-38.01	30.54	

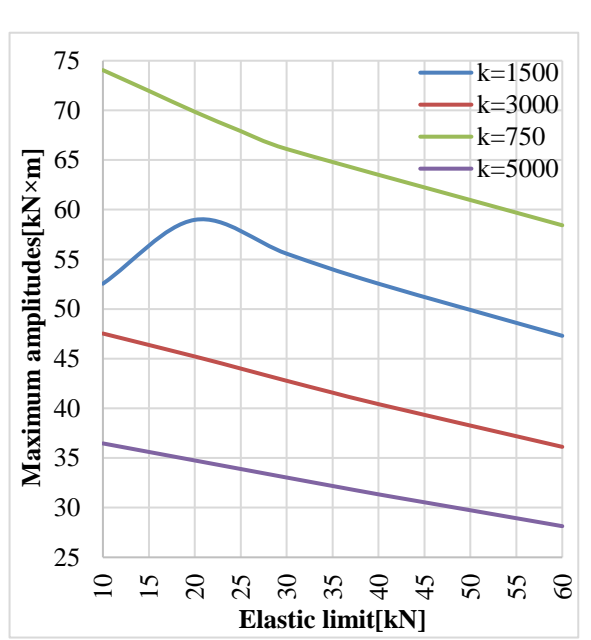


Figure 55 –Bending moment variation as a function of the device characteristics

Regarding the bending moments in the anchorages, the same observations can be applied as for the displacements, with the best results for the stiffer device and the larger elastic bearing. Compared to the reference value of 91 kN \times m, values of 66 kN \times m, 47 kN \times m, 36 kN \times m and 28 kN \times m are reached, respectively. It is not desired to analyze cases with a higher yield strength, because they would lead to too high forces in the devices, which would give unacceptable bending moments in the area of attachment of the device.

However, the most important performance criterion for these devices is that of damping. Next, results are presented in terms of the energy dissipated by the devices and the percentage of critical damping achieved at the free-vibration stage.

Stiffnes s	\mathbf{f}_{el}	Dissipated energy			Damping
kN/m	[kN]	Forced vibration [kJ]	Free vibration [kJ]	Total [kJ]	%
k=750	15	124.81	41.14	165.95	0.411%
	20	140.79	37.20	177.99	0.411%
	25	145.35	30.43	175.78	0.400%
	30	141.16	23.23	164.40	0.386%
k=1500	10	160.61	23.60	184.21	0.393%
	20	140.42	42.89	183.31	0.428%
	30	163.72	35.29	199.00	0.426%
	40	160.61	23.60	184.21	0.393%
	60	115.58	8.35	123.94	0.346%
k=3000	20	113.05	36.10	149.15	0.417%
	25	129.54	35.48	165.02	0.427%
	30	141.21	33.09	174.29	0.431%
	35	148.08	29.60	177.67	0.428%
	40	150.60	25.38	175.98	0.417%
k=5000	30	110.67	26.06	136.73	0.415%
	35	117.91	23.66	141.57	0.417%
	40	122.00	20.65	142.64	0.413%
	45	123.33	17.41	140.75	0.389%

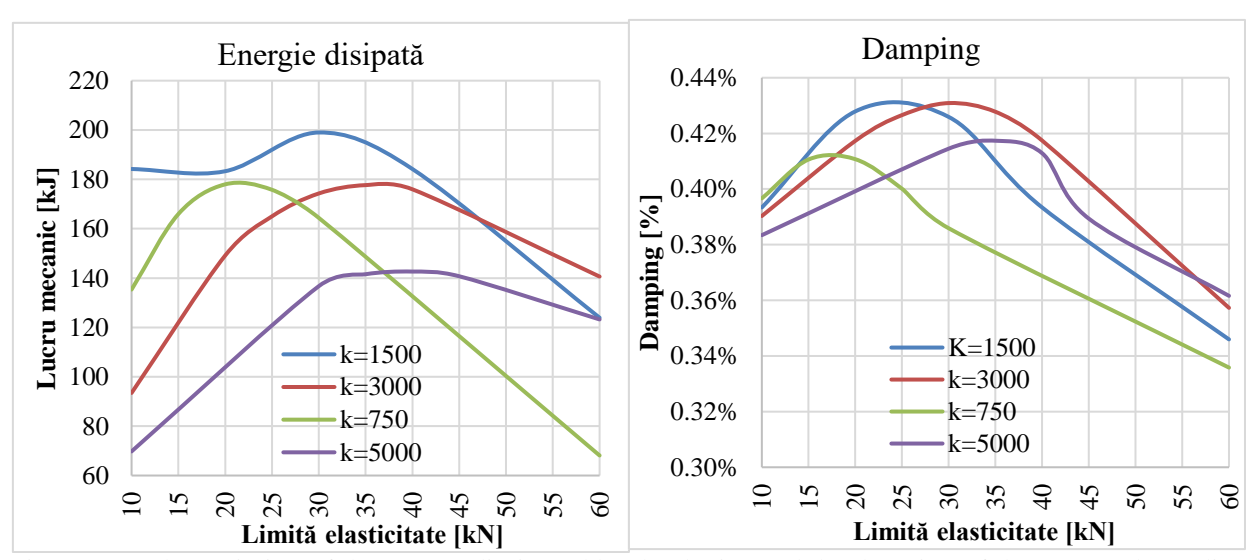


Figure 56 – The variation of the energy dissipated by the device and the damping of the system depending on the characteristics of the elastomer

.

By analyzing the obtained results, it is observed that neither the most rigid devices studied nor the most flexible ones give the best results. The optimal results were obtained for the device with stiffness $k=1500~kN\times m$ and elastic limit of 20 kN which corresponds to a total dissipated energy of 200kN and a damping of 0.428%, respectively the one with $k=3000~kN\times m$ and bearing elastic up to 30 kN with a total dissipated energy of 178 kN×m and a damping of 0.431%.

For a better understanding of how this type of device works, the force-displacement hysteresis curve for the optimal device is presented below.

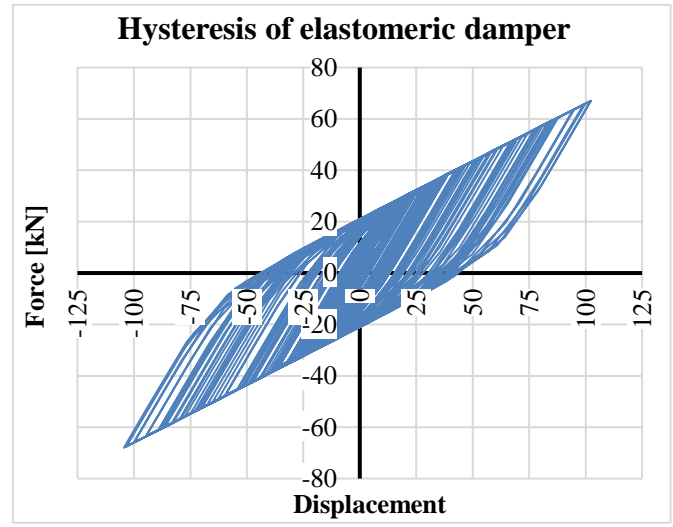


Figure 57 –Force-displacement curve in elastomeric damper

The high efficiency interval of this energy dissipation mechanism is not as strict as in the case of viscous dampers, having a wider range of parameters that generate good results. However, it should also be taken into account that the efficiency of the viscous ones is at least 2 times higher in all respects compared to the elastomeric ones.

IV. CONCLUSIONS

All vibration damping systems reduce the harmful effects on bridge piers and their elements to some extent, provided they are correctly tuned. An incorrect dimensioning can make the implementation of these devices have no effect or even further damage on the structure.

Attaching the tuned masses led to a reduction by half of the amplitudes of the forced vibrations, both in terms of displacements and stresses in the anchorages, but had no noticeable influence on the damping. This method can be used successfully when the exact critical period to be avoided is known. Due to the uncertain nature related to the various external phenomena that induce oscillations in the cables, this method is difficult to apply, especially in the case of cables longer than 300m. Recent research in the field of viscous or frictional masses is proposing new prototypes that could prove to be a very effective solution for any type of cable.

The attachment of cross ties showed a reduction in terms of deformations by about 30% and stresses in the anchorages by only 15%, without having any impact on the damping of the system. For a more favorable response of the cable, it is necessary to connect several stays together, each with different dynamic characteristics. In addition, in order to reduce the forces in the anchorages, it is necessary to install ties in the vicinity of each anchorage, since the impact of the one on the opposite end turned out to be insignificant.

The attachment of the viscous dampers to the stays proved to be the most effective of the situations studied, leading to the decrease of the maximum amplitudes by about 20%, the decrease of the stress differences in the anchorages by up to 73% and the increase of the damping of the system by almost 3 times. It is noted that these performances were achieved at different viscosity coefficients for each load case. It is recommended to favor maximum damping over other performance criteria. The determination of the optimal viscosity for each device must be carried out by special analyzes, simplified formulas focused on target vibration modes being insufficient.

Attaching the elastomeric dampers on the cable reduced the maximum displacements by approximately 13%, decreased the forces in the anchorage by up to 44%, and increased the

damping of the system by 48%. However, the performance of this system for the analyzed stay is quite low. In forced vibration conditions, the efficiency is estimated to be acceptable for cables up to 200-250m.

The practice at the international level for the design of cable-stayed bridges recommends that the Scruton number has a minimum value of 10 for the vibration stability of the cables, which corresponds, for the adopted cable-stayed section, to a minimum percentage of the critical damping of 0.6%. In the proposed design situations, only viscous dampers were able to satisfy this safety criterion. This result, however, does not exclude the possibility of using other types of systems in other cases.

The performance and safety criteria imposed on engineers today for bridge structures with large and very large spans crossed by cable stayed bridges require the implementation of vibration dampening devices on the cables. They greatly reduce maintenance costs and increase the life of the structure.

BIBLIOGRAPHY

- ^[1]Walter Podolny, Jr., Ph. D. and John B. Scalzi, Sc. D. *Construction and Design of Cable-Stayed Bridges* Second Edition, John Wiley & Sons, New York 1986
- [2]Rene Walther, B Houriet Cable stayed bridges, Thomas Telford Publishing, Londra 1999
- [3] Niels J. Gimsing, Christos T. Georgakis *Cable Supported Bridges, concept and design*, John Wiley & Sons, New York 1997
- ^[4]Y. L. Xu, L. Y. Wang *Analytical study of wind-rain induced cable vibration: SDOF model,* Journal of Wind Engineering, Hong Kong, 2003
- [5] Masaru Matsumoto Review of Bridge Cable Vibrations in Japan, Kyoto University, 2006
- ^[6]Marius Giuclea, Tudor Sireteanu, Danut Stanicioiu, Charles W. Stammers *Modelling of magnetorheological damper dynamic behaviour by genetic algorithms based inverse method*, Bucureşti, 2004
- ^[7]W. J. Wu, C. S. Cai, S. R. Chen Experiments on reduction of cable vibration using MR dampers, Delaware, DE
- ^[8]Marcin Maslanka, Bogdan Sapinski *Experimental study of vibration control of a cable with an attached MR damper*, Varșovia, 2007
- ^[9]F. Naeim, J. M. Kelly Design of Seismic Isolated Structures: From Theory to Practice, John Wiley & Sons, New York 1999
- [10] Eth Zurich Mitigation of stay cale vibrations with magnetorheological dampers, Zurich, 2010 [11] Joseph A. Main Modelling the vibrations of a stay cable with attached damper, Baltimore, 2002
- ^[12]X. Y. Wang, Y. Q. Ni, J. M. Ko, Z. Q. Chen Optimal design of viscous dampers for multimode vibration control of bridge cables, Hong Kong, 2004
- ^[13]Habib Tabatabai, Armin B. Mehrabi *Vibration supression measures for stay cables*, Illinois, 2003
- [14] Erik A. Johnson, B. F. Spencer, Yozo Fujino Semiactive damping of stay cables, ASCE 2007
- [14] Cataloage și lucrări Maurer Sohne
- [15] Cataloage și lucrări Freyssinet
- [16] www.wikipedia.org